A new methodology to train fracture network simulation using Multiple Point Statistics

Pierre-Olivier BRUNA[(1)*], Julien STRAUBHAAR[(2)], Rahul PRABHAKARAN[(1, 3)], Giovanni BERTOTTI[(1)], Kevin BISDOM[(4)], Grégoire MARIETHOZ[(5)], Marco MEDA[(6)].

(1) Department of Geoscience and Engineering, Delft University of Technology, Delft, the Netherlands.
(2) Centre d'hydrogéologie et de géothermie (CHYN), Université de Neuchâtel, Emile-Argand 11, CH-2000 Neuchâtel.
(3) Department of Mechanical Engineering, Section of Energy Technology, Eindhoven University of Technology, Eindhoven the Netherlands.
(4) Shell Global Solutions International B.V., Grasweg 31, 1031HWAmsterdam, The Netherlands
(5) University of Lausanne, Institute of Earth Surface Dynamics (IDYST) UNIL-Mouline, Geopolis, office 3337, 1015 Lausanne, Switzerland
(6) ENI Spa, Upstream and Technical Services, San Donato Milanese, Italy.

* Corresponding author, p.b.r.bruna@tudelft.nl

Keywords: geostatistics, multiple training images, probability map, fracture networks, stress-induced fracture aperture, outcrop.

Abstract

Natural fracture network characteristics can be known from high-resolution outcrop images acquired from drone and photogrammetry. These outcrops might also be good analogues of subsurface naturally fractured reservoirs and can be used to make predictions of the fracture geometry and efficiency at depth. However, even when supplementing fractured reservoir models with outcrop data, gaps in that model will remain and fracture network extrapolation methods are required. In this paper we used fracture networks interpreted in two outcrops from the Apodi area in Brazil to present a revised and innovative method of fracture network geometry prediction using the Multiple Point Statistics (MPS) method.

The MPS method presented in this article uses a series of small synthetic training images (TIs) representing the geological variability of fracture parameters observed locally in the field. The TIs contain the statistical characteristics of the network (i.e. orientation, spacing, length/height and topology) and allow representing complex arrangement of fracture networks. These images are flexible as they can be simply sketched by the user.

We proposed to use simultaneously a set of training images in specific elementary zones of the Apodi outcrops defined in a probability map in order to best replicate the non-stationarity of the reference network. A sensitivity analysis was conducted to emphasize the influence of the conditioning data, the simulation parameters and the used training images. Fracture density computations were performed on the best realisations and compared to the reference outcrop fracture interpretation to qualitatively evaluate the accuracy of our simulations. The method proposed here is adaptable in terms of training images and probability map to ensure the geological complexity is accounted for in the simulation process. It can be used on any type of rock containing natural fractures in any kind of tectonic context. This workflow can also be applied to the subsurface to predict the fracture arrangement and fluid flow efficiency in water, heat or hydrocarbon fractured reservoirs.

I] Introduction

I.1 The importance of the prediction of fracture network geometry

~~Fractures are ubiquitous in Nature and are known to impact fluid flow and fluid storage~~ Fracture are widespread in Nature and depending on their density and their aperture, they might have a strong impact on fluid flow and fluid storage in water (Berkowitz, 2002; Rzonca, 2008), heat (Montanari et al., 2017; Wang et al., 2016) and hydrocarbon reservoirs (Agar and Geiger, 2015; Lamarche et al., 2017; Solano et al., 2010) They are typically organised as networks ranging from nanometre to multi-kilometre scale (Zhang, 2016), and

present systematic geometrical characteristics (i.e. type, orientation, size, chronology, topology) that are determined from specific stress and strain conditions. T~~hese conditions are typically well known~~ These conditions have been used to derive concepts of fracture arrangements in various tectonic contexts and introduced the notion of geological fracture-drivers (fault, fold, burial, facies). Based on these drivers it is possible to some extent to predict reservoir heterogeneity ~~in folded (Suppe, 1983, 1985; Tavani et al., 2015; Watkins et al., 2017), faulted (Faulkner et al., 2010; Matonti et al., 2012; Micarelli et al., 2006) and burial-related contexts (Bertotti et al., 2017; Bisdom, 2016) and have been used to derive concepts of fracture arrangements. These concepts are currently used~~ and to define potential permeability pathways within the rock mass (Lamarche et al., 2017; Laubach et al., 2018). ~~Despite the existence of these concepts, fracture networks generally present an intrinsic complexity (e.g. variability of orientation, local occurrence of new fracture family, change of topology relationships) due, among others, to local variability of the orientation and magnitude of stresses. This makes fractures hard to predict. Moreover, fractures in subsurface reservoirs are largely unknown due to their sub-seismic size and to the scarcity of available data, which is generally limited to borehole information.~~ Despite the existence of these concepts, a range of parameters including fracture abutment relationships as well as height/length distributions cannot be adequately sampled along a 1D borehole and are mainly invisible on seismic images. In addition, fracture networks may present a spatial complexity (variability of orientation or clustering effect) that is also largely unknown in the subsurface. (Long and Witherspoon, 1985) and (Olson et al., 2009) showed how those parameters impact the connectivity of the network and consequently affect fluid flow in the subsurface. In outcrops, the fracture network characteristics can be observed and understood directly. Consequently, outcrops are essential to characterize fracture network attributes that cannot be sampled in the subsurface, such as length or spatial connectivity.

I.2 Surface rocks as multiscale reservoir analogues

In this context, the study of outcrop analogues is one of the few ways to constrain the architecture of fracture networks (Bisdom et al., 2014; Bruna et al., 2017; Council, 1996; Lamarche et al., 2012; Lavenu et al., 2013). Outcrops can be considered as a natural laboratory where the structural reality can be observed and quantified at various scales. At the small – measurement station – scale (order of 10's m), fracture type, chronologies and topology relationships can be characterised using classical ground-based structural geology method such as scanlines (Lavenu et al., 2013; Mauldon et al., 2001). At the intermediate – outcrop – scale (order of 10^2's m), length of fractures and geometry variability can be qualified and quantified using unmanned aerial vehicles (UAV - drones). Working on outcrops allows an understanding of the geological history of the targeted area and eventually to decipher how, when and where fractures were developed. In addition, outcrops constitute an efficient experimental laboratory where some of properties of the fracture network (i.e. fracture distribution, apertures, permeability and fluid flow behaviour) can be known and modelled (Bisdom et al., 2017). At the large – reservoir – scale (order of $10^{3\text{-}4}$m) satellite imagery and geophysical maps provide the characterisation of the 100's of meter long objects such as large fracture systems or faults.

However, not every outcrop can be considered as a good analogue for the subsurface. (Li et al., 2018), in their work on the Upper Cretaceous Frontier Formation reservoir, USA, observed significant differences in the fracture network arrangement in subsurface cores compared to an apparent good surface analogue of the studied reservoir. In the subsurface, fractures appeared more clustered than in the outcrop where the arrangement is undistinguishable from random. The origin of these differences is still debated but these authors suggest that alteration (diagenesis) or local change in pressure-temperature

conditions, may have contributed to the observed variability. The near-surface alteration processes (exhumation, weathering) may also contributed to misinterpretations of the characteristics of the network. In this case, one should be particularly careful while using observed networks to make geometry or efficiency (porosity, permeability) predictions in the subsurface. Therefore, the application to the subsurface of the characteristics observed in the outcrop is not always straightforward or even possible, and may lead to erroneous interpretations. Relatively unbiased signals such as stylolites or veins and particular geometric patterns might be a trustful basis to show that the studied outcrop can be, to some extent, compared to the subsurface.

I.3 Modelling approaches classically used to model fracture network geometries

The widely used discrete fracture network (DFN) stochastic modelling tools ~~are providing~~ provide statistical representation of fracture networks constrained generally by univariate and random distribution of orientation, size, spacing and density/intensity data (Bisdom et al., 2014; Bisdom et al., 2017; Huang et al., 2017; Panza et al., 2018). ~~The generated models implicitly follow a local stationarity hypothesis suggesting the invariance of all of the generated statistics by translation in the simulated domain~~ The generated models follow a local stationarity hypothesis. This implies that the statistics used during the simulation are constant in the defined area of interest (Deutsch and Journel, 1997; Gringarten and Deutsch, 1999; Gringarten and Deutsch, 2001; Journel and Zhang, 2006). (Liu et al., 2009), highlighted the implicit randomisation that conventional DFN models produce and demonstrated that parameters like fracture connectivity are poorly considered in these representations. In addition, it is generally admitted that discrete realisations of thousands of fractures objects at the kilometre scale are computationally very demanding and often even impossible (Jung et al., 2013). Some authors attempted to use a pixel-based method to try to predict fracture

network geometries. (Bruna et al., 2015), used a dense hydrogeological borehole survey sampling a Lower Cretaceous aquifer in the SE of France to define fracture facies and to model their distribution with two-points geostatistics. In this case, the amount of available data and their consistency helped to provide realistic results. However, far from conditioning data (i.e. boreholes) the fractures simulation are poorly constrained.

The work of (Hanke et al., 2018) uses a directional semi-variogram to quantify fracture intensity variability and intersection density. This contribution provides an interesting way to evaluate the outputs of classical DFN approaches but requires a large quantity of input data that are not always available in the subsurface. To geologically represent the fracture network geometry in various contexts, an alternative method has to be developed. This innovative method needs to i) explicitly predicts the organisation and the characteristics of multiscale fracture objects, ii) takes into consideration the spatial variability of the network and iii) requires a limited amount of data to be realised.

~~The second paragraph of the comment was modified in the reference list.~~

I.4 Multi-point statistics as an alternative to classic DFN approaches

Since (Liu et al., 2002), few authors highlighted the potential of using multi-point statistics (MPS) to generate realistic fracture networks (Chugunova et al., 2017; Karimpouli et al., 2017). (Strebelle, 2002) showed how the MPS are able to reproduce any type of geological heterogeneities of any shape at any size as long as they present a repetitive character. This characteristic seems particularly well adapted to predict the geometry of a fracture network. The MPS method uses training images (TI) to integrate conceptual geological knowledge into geostatistical simulations (Mariethoz, 2009). The TI is a grid containing geological patterns that are representative of a certain type of geological structure, type and arrangement. The TI can be considered as a synthetic model of the geological heterogeneity (i.e. all the elements

characterising a geological object) likely to occur in a larger domain (i.e. reservoir, aquifer, outcrop). The TI must include the possible range and shape of the geobodies that the geoscientist intends to model, as well as the relationship these geobodies have with each other (Mariethoz, 2009; Strebelle, 2002).

I.5 Objectives and contents of this research

In this paper we propose a MPS workflow considering the geological variability of the fracture network geometry ~~variability over full outcrops and a methodology~~ in outcrops (size order of 100m) and a methodology on how to use this method at the reservoir scale. The approach is based on the direct sampling method (Mariethoz et al., 2010) and uses multiple training images for a single realisation (Wu et al., 2008). The concept of the probability map has been revised here to define where a training image should be used in the simulation grid. Our outcrop-based simulations also take into account "seismic-scale" objects (i.e. object longer than 40m) considered as hard conditioning data. The proposed workflow is tested on outcrops considered as analogues of the Potiguar Basin, Brazil where fracture network have been previously characterised and interpreted from drone imagery (Bertotti et al., 2017; Bisdom, 2016). Uncertainties were evaluated by comparing original outcrop interpretation (done manually by a geologist) with the geometrical characteristics of the network generated from MPS. To evaluate the quality of the simulations, ~~we computed mechanical and hydraulic apertures in outcrop fracture interpretation and on the obtained stochastic models~~ we computed density maps in outcrop fracture interpretation and on selected stochastic models. The proposed approach is innovative and provides a quick and efficient way to represent fracture network arrangements at various scales.

II] Methodology

II.1 The direct sampling method

The direct sampling method (DS) was introduced by (Mariethoz et al., 2010). Figure 1, synthesizes the DS modelling process developed thereafter. The method requires a simulation grid where each node is initially unknown and called $\boldsymbol{x}$, a training image grid (TI) where each node is known and called $\boldsymbol{y}$ i.e. V(y) is defined where V is the variable of interest (e.g. facies value). The simulation proceeds as follows. First, the set of conditioning data (if present) is integrated in the simulation grid. Then, each remaining unknown node $\boldsymbol{x}$ is visited following a random or defined path, and simulated as follows. 1) The pattern $\boldsymbol{d_n(x)} = \boldsymbol{(x_1,V(x_1)),\ldots,(x_n,V(x_n))}$ formed by the at most **n** informed nodes the closest to $\boldsymbol{x}$ is retrieved. Any neighbour $\boldsymbol{x_i}$ of $\boldsymbol{x}$ is either a previously simulated node or comes from the conditioning data set. The lag vectors $\boldsymbol{h_i} = \boldsymbol{x_i}\text{-}\boldsymbol{x}$ define the geometry of the neighbourhood of $\boldsymbol{x}$. The combination of the value and position of $\boldsymbol{x}_i$ defines the data event or pattern $\boldsymbol{d_n(x)}$. 2) Then, the TI is randomly scanned to search for a pattern $\mathbf{d_n(y)}$ similar to $\mathbf{d_n(x)}$. For each scan node $\boldsymbol{y}$, the pattern $\boldsymbol{d_n(y) = (y_1,V(y_1)),\ldots,(y_n,V(y_n)),}$ where $\boldsymbol{y_i}=\boldsymbol{y}+\boldsymbol{h_i}$, is compared to $\mathbf{d_n(x)}$ using a distance (Meerschman et al., 2013). When the distance is lower than an acceptance threshold ($\boldsymbol{t}$) defined by the user or if the proportion of scanned nodes in the TI reaches a maximal fraction (f) defined by the user, the scan is stopped and the value of the best candidate $\boldsymbol{y}$ (pattern with the minimal distance) is directly attributed to $\boldsymbol{x}$ in the simulation grid (i.e. $\boldsymbol{V(x) = V(y)}$).

As the DS method does not use a catalogue of all possible patterns found in the TI, it is extremely flexible and in particular allows taking into account both categorical and continuous variables and managing multivariate cases, provided that the pattern distance is suitable. In this paper we are using the DeeSse version of the direct sampling code (Straubhaar, 2017).

II.2 Multiscale fracture attributes

To evaluate how the direct sampling method is dealing with the fracture network, the present experimentation is based on outcrop data ~~(reference)~~ where the present-day "structural reality" is observable at various scales. Pavements (i.e. horizontal surfaces in the order of 10^2 m scale) were targeted because these objects contain important information that is not always accessible with standard vertical outcrops (Corradetti et al., 2017a; Corradetti et al., 2017b; Tavani et al., 2016) or with classic geophysical imagery. Pavement sizes allow the user to interpret and localise fracture patterns variability (Bruna et al., 2018). For instance, clusters of fractures (i.e. local increase of the fracture density) can be identified by the interpreter. Pavements also allow to obtain quantitative data on fracture lengths, which are usually difficult to get in vertical cliff. In the subsurface, data can be provided by geophysical 3D maps and fracture attribute detection tools (Chopra and Marfurt, 2007; Somasundaram et al., 2017). However, these tools are not always available and detect the longer lineaments only ~~(e.g. > 50 m long depending on the resolution of the imagery).~~

Working with pavements constitutes an asset as small-scale investigation can be conducted in key zones of the outcrop (i.e. in folded areas, each compartment or dip domain of the fold should be imaged and investigated in detail) where the gathered data will help to calibrate larger scale information. Classical fieldwork methods (observation and characterisation, measurements, statistical analyses, sampling) help interpreting fracture families and are essential to constrain larger scale observation.

In this study, UAV-based photogrammetry is used to obtain an orthorectified mosaic and 3D digital outcrops models (Bemis et al., 2014; Claes et al., 2017; Vollgger and Cruden, 2016). The scale of these images is an intermediate between the scale of measurement station and that of satellite imagery. Digitization of fracture traces, geological contacts, sedimentary structures and structural domain boundaries are currently processed by hand and represent a considerable time investment. In this contribution, fractures were interpreted in orthomosaic

images with the help of GIS software. Length, azimuth, fracture family proportions and fracture density statistics were extracted from the interpretation. In addition, a series of measurement station (area of about 2 × 2 m) information was acquired and compared with the dataset from the drone imagery in order to align interpretations and provide coherent fracture history.

II.3 Training images, conditioning data and probability maps

- **Training images**

Training images (TI) are the base input data of the MPS simulation. Building them is a critical step to succeed a realisation (Liu et al., 2009). The TI is a pixelated image based on a local interpretation of a geological phenomenon (i.e. an interpreted photography taken from a local zone of interest in the field) or digitised by a geologist and based on geological concepts (Strebelle, 2002). These images should synthesise all of the recognized geological parameters that characterise the area to simulate. This implicitly means that the proportion of facies carried by the TI, will be reproduced into the simulation grid but this also requires extensive pre-processing work (see example of TIs in figures 5, 6, 9 and 10). To manage this complexity, ~~we propose to~~ we used multiple training images where facies proportion and geometrical distribution can vary. Hence, each TI has a local impact on the simulation. Moreover, in our approach fractures sets are grouped in facies in the TI, based primarily on their orientation and possibly on their length or additional parameters defined by the user. The fractures classification helps reproducing patterns and simplifies the process of building the TI.

- **Conditioning data**

One limitation of the MPS methods is the tendency to disconnect long continuous objects (i.e. typically fractures, (Bruna et al., 2017). To manage this issue, ~~longer~~ long fractures can be

identified and incorporated into the simulation as conditioning data. As per the training images, such data can be integrated as pixelated grids. They may come from satellite imagery or they can be interpreted from gravity or magnetic surveys or from 3D seismic imagery (Magistroni et al., 2014).

- **Probability map**

The direct sampling method can be used with multiple training images. In this situation, the user provides a set of TIs, and for each TI a probability map defined on the simulation grid, giving at each node the probability to use that TI. The pixel-wise sum of these maps should then be equal to one in every node. If each TI corresponds to a partition of the area of interest, with for each TI one elementary zone, covering the whole simulation grid, the probabilities in the map are set to one for specific TI and to zero for the other ones.

The probability map comes from a simple sketch (i.e. a pixelated image) given by the MPS user. It is based on the geological concepts or interpretations that define the geometry variability over the simulated area and that allow a partition of the outcrop. In each of the zones defined in the area of interest, the simulated property will follow the intrinsic stationary hypothesis (Gringarten and Deutsch, 2001; Journel and Zhang, 2006; Journel, 2005) but the entire domain will be non-stationary.

While working on outcrops, the partition of the area of interest can be determined based on observations. For instance, when the fracture network interpreted from outcrop images is available, the geologist can visually define where the characteristics of the network are changing (fracture orientation, intensity, length, topology) and draw limits around zones where the network remains the same. However, in other cases outcrops or subsurface observations could be discontinuous between observation sites. If the data are sparse and come mainly from fieldwork ground observations or boreholes, the use of alternative statistical approaches can help to provide a robust and accurate partition of the area of

interest. The work of (Marrett et al., 2018) interprets the spatial organisation of fractures using advanced statistical techniques such as normalized correlation count and weighted correlations count, on scanlines collected in the Pennsylvanian Marble Falls Limestone. In their approach, the periodicity of fracture spacing (clustering) calculated from the mentioned techniques is evaluated using Monte Carlo to quantify how different the fracture networks are from a random organisation. These approaches can be highly valuable during the process of building a probability maps when less data are available. ~~comes from a simple sketch (i.e. a pixelated image) given by the MPS user. It is based on geological concepts that define the geometry variability over the simulated area. In each of these areas the simulated property will follow the intrinsic stationary hypothesis (Gringarten and Deutsch, 2001; Journel and Zhang, 2006; Journel, 2005) but the entire domain will be non-stationary.~~ The probability maps provide a large-scale framework that may be refined and modified with additional data such as measurement stations or drone surveys coming from surface exploration or wells data containing fracture network information.

II.4 Testing the simulated network: from pixels to segments

MPS realisations are produced as pixelated images. To evaluate the resulting fracture network, pixels alignments corresponding to fractures are extracted as discrete straight-line objects defined by a starting and an ending x, y coordinates ~~using a custom MATLAB routine~~. Fractures are separated from the background and in different sets by automatic image classification methods. On grayscale images, this is obtained by multilevel image thresholding through the Otsu's method (Otsu, 1979). On color images, fracture sets are classified based on their color components with the k-means clustering algorithm built in MATLAB (Lloyd, 1982), ~~on images previously converted to the perceptually uniform Lab color space.~~ Image classification gives in output a series of binary images, one for each

fracture set, where lineaments are represented as foreground (Kovesi, 2000). ~~The foreground segments are finally fitted with straight lines using the *lineseg.m* algorithm by, which gives in output a list of starting and ending point coordinates for each fracture set.~~

III] Results: test case on analogues of the Potiguar Basin, E Brazil

III.1 Geological setting

The Potiguar Basin is a rift basin located in the easternmost part of the Equatorial Atlantic continental margin, NE Brazil (fig. 2). The basin is found both onshore and offshore (fig. 2). The basin was generated after the initiation of the South American and African breakup during the Jurassic - Early Cretaceous times. It was structured by a first NW-SE extension stage latterly rotating to an E-W extensional direction (Costa de Melo et al., 2016). The rift basin displays an architecture of horsts and grabens striking NE-SW and bounded towards the east and south by major faults systems (de Brito Neves et al., 1984), fig. 2). The Potiguar Basin displays three sedimentary sequences deposited since the early Cretaceous times (i.e. syn- and post rift depositions). The last post-rift sequence was deposited from the Albian and encompasses the Cenomanian-Turonian Jandaíra Formation. This formation consists of up to 700 m thick bioclastic calcarenites and calcilutites deposited in transgressive shallow marine environment. The stress field affecting the Jandaíra Formation during the Campanian to the Miocene compression was oriented N-S (Bertotti et al., 2017). From the Miocene to the Quaternary the onshore part of the Potiguar basin was uplifted. Synchronously, a new stress field was established trending to a NW-SE direction (Reis et al., 2013).

III.2 Outcrop data

The area of interest measures 2.1 × 1.3 km and is located about 25 km NE of the city of Apodi in the Rio Grande Do Norte state (fig. 2). It contains two outcrops AP3 and AP4 (Bertotti et

al., 2017; Bisdom, 2016), fig. 2) here defined respectively as 600 × 300 m and 400 × 500 m large pavements localized in the Jandaíra Formation. AP3 and AP4 crop out as pavements with no significant incision. The outcrops are sparsely covered by vegetation and consequently they present a clear fracture network highlighted by karstification. In 2013, images of AP3 and AP4 were acquired using a drone (Bisdom, 2016) and processed using the photogrammetry method. Two high-resolution ortho-rectified images of these pavements (centimetre-scale resolution) were used to complete fracture network interpretation and to extract fracture parameters. In AP3, 775 lineaments were traced (fig. 3) and in AP4, 2593 (fig. 4). These lineaments are grouped in this article over the general term "fractures". For each of these outcrops three fractures sets were identified: set1 striking N135-N165, set2 striking N000-N010/N170-N180 and set 3 striking N075-N105. Fractures falling outside of these ranges were not considered in the input data. Consequently, in AP3 we considered 562 only (out of 775 fractures traced in the pavement) and in AP4 we considered 1810 only out of 2594 fractures. In addition, ground-based fieldwork was conducted in AP3 and AP4 to understand the structural history of the area and to calibrate the interpretation conducted on the drone aerial photography (Van Eijk, 2014). General location and fracture data are presented in figure 3 and 4 and in table 1.

In AP3, sets 1 and 2 are evenly distributed over the pavement. However, they present intrinsic intensity variability in the area of interest. Set 3 is mainly expressed in distinct regions of the outcrop. Small-scale investigations (conducted on measurement stations in the outcrop) allowed associating set 3 with stylolite and sets 1 and 2 to veins. In addition, sets 1 and 2 present evidences of shear movements and are then considered as a conjugate system.

In AP4 small-scale investigations highlight the same characteristics as the ones observed in AP3. Although the conjugate system (set 1 and set 2) is less developed there than in AP3. It is also notable that more crosscutting relationships were observed in AP4 compared to AP3.

III.3 Input data for MPS simulation

~~AP3 illustrates the effect of conditioning data and of simulation parameters in the stochastic realisations.~~ To evaluate the effect of conditioning data, results of two simulations were compared, with and without conditioning data. The sensitivity of simulation parameters was investigated by varying i) the number of neighbours defining patterns (data events $\boldsymbol{d_n}$), ii) the acceptance threshold ($\boldsymbol{t}$) defining the tolerance the algorithm authorises to find a matching data event in the simulation grid (Mariethoz et al., 2010) and iii) the fraction of the TI to be scanned during the simulation process to search for data events. Results of this sensitivity analysis help to propose the best possible simulation for AP3 and to optimise the choice of input parameters for AP4 fracture simulation.

AP3 presents intrinsic fracture network geometry variability. This observation emphasizes that averaging fracture parameters on the entire domain is not well suited to represent the complexity of the network. We observed that the length of fracture per sets and the density of fractures are parameters that vary the most here. The analysis of these variations allow to partition AP3 and AP4 in elementary zones and to synthesize the fracture network characteristics in each of these domains. The following section defines how the TI, ~~PM~~ probability map and conditioning data were built.

- **Partitioning, training images and probability map for AP3 and AP4**

We divided AP3 in 5 elementary zones (EZ) based on visual inspection of the pavement (fig. 5A-B). The number of fractures per EZ is synthesized in the figure 5. The proportion of fracture per elementary zone is available in table 1. A limited part of the fractures belong to two neighbours elementary zones. This issue is quantified in table 1.

A probability map with sharp boundaries (fig. 5B) was created for AP3. Sharp boundaries are justified by the variability of the network geometry, which is known from the visual

inspection of the interpreted image. Smooth transitions could also be defined (see discussion). The input data to build the probability map is an image of the partition of the area of interest containing the different outcrops. In this image, the indexed zones (elementary zones EZ) are characterised by a distinctive colour.

~~The goal of this research is to show that MPS is able to accurately reproduce an existing fracture network (interpreted on AP3 outcrop) from small and simplified sketches (training images) representing what the network should look like in each elementary zone.~~ At the scale of a reservoir where some outcrops analogues and fracture tracing may be available, the "interpreted reality" of the network can be directly used as a training image. We chose to ignore the tracing and to rely on parameters that are classically available without having access to drone images of an entire outcrop (i.e. orientation, spacing, abutment) and to compare the interpretation with the simulated network. In that respect fracture orientation were averaged to a single value. Hence, set 1 strikes N150, set 2 strikes N000 and set 3 strikes N090. According to the outcrop partitioning, five training images were created (fig. 5C). In each training image, three facies corresponding to the three fracture sets were created. Set1 (N090) is green, set 2 (N150) is red and set 3 (N000) is blue (fig. 5C). The topology is a crucial problem in fracture simulations because it influences the connectivity of the network. In the MPS simulations the abutments are particularly well reproduced as they represent singular pixels arrangements that are efficiently taken into account. However, crosscutting relationships imply the use of a different facies at the intersection locus. This method respects and reproduces intersections during the simulation process. In AP3, the analysis of the topology relationships showed three main crosscutting interactions:

- Long N150 crosscut long N000 fractures (conjugated sets)
- N000 crosscut N090
- N150 crosscut N090

To take into account these topological parameters a different facies colour was attributed to the crosscutting locus (the crossing facies, fig. 6). When the MPS realization will be later discretized, the younger fractures will be truly represented as continuous segments. The older fractures will be cut in pieces but their alignment will be, in most of the case, maintained during the simulation process.

- **Dimensions of the simulation grids and of the training images**

The dimensions of the simulation grid for AP3 and of each training image (in pixels) are shown in fig.5. The number of pixels is automatically determined by the size of the original drawing made by the geologist.

The size of the input training image does not generally influence the simulation. However, it has to be chosen sufficiently large with respect to the complexity of the patterns in order to get reliable spatial statistics. The DS method tends to identify patterns (i.e. $\boldsymbol{d_n}$'s see above) in the TI and to paste the central node of them into the simulation grid. However, at a constant resolution and specifically for fractures patterns, it is likely that a 50 × 50 m training image will carry more complexity and variability than a 10 × 10 m one. This parameter should be taken into consideration when starting digitizing training images, especially when spacing between fractures is not consistent across the simulation grid.

- **Long fractures conditioning**

Because the MPS method has the tendency to cut long individual segments into smaller pieces, the fractures longer than 40 meters – the ones visible from satellite/drone imagery in AP3 – where isolated and considered as hard conditioning data (fig. 5D). This threshold was arbitrarily determined from the dataset we have. In AP3, less than 8% of the fractures are longer than 40 m.

In AP3, long fractures belong only to the sets oriented/striking N000 or N150 (fig. 5D). 18 N000 fractures (3% of the whole) and 30 N150 fractures (5% of the whole) were digitized and integrated as conditioning data in the simulation.

III.4 Outcrop scale simulations

III.4.1 Impact of conditioning data on AP3 simulations

In AP3, the 48 long fractures were manually digitized and imported into the simulation grid as categorical properties to be considered as hard conditioning data during the MPS simulation process. The MPS simulation is consequently in charge of stochastically populating the smaller factures within the grid.

Results of the influence of these data are presented in figure 7. The principal simulation parameters in the considered scenarios (with and without conditioning data) were set up identical (constant acceptance threshold (5%), constant percentage of scanned TI (25%) and constant number of neighbours (50)).

Results showed that the realisation without conditioning data creates 20% less fracture than the original outcrop reference. The simulation with conditioning data creates 9% less fractures than AP3, which makes the simulation satisfactory. It is also remarkable that the non-constrained simulation represents only 23 fractures above 40 meters (compared to the 48 long fractures interpreted on the AP3 outcrop). In this simulation the long fractures are essentially located in the zone 3 of the outcrop. Because the simulation is a stochastic process, the location of the long fractures is randomly determined in the absence of hard conditioning data. Considering hard-conditioning data also gives a more realistic representation of the fracture network.

III.4.2 Sensitivity analysis on the AP3 simulation parameters

- **Simulation parameter set-ups, duration and analyses conducted on the results**

Simulation parameters were varied for each simulation in order to emphasize their effect on each realisation. One realisation per test was performed during this analysis. The goal of this analysis is to show how the different parameters influence the reproduction of fracture segments and not to evaluate how good is the matching between the simulation and the reference.

The MPS realisations are pixelated images. The sensitivity analysis is based on the discrete segments extracted from these pixelated images (see II.4). All of the simulations present a variable percentage of segment lengths that are below the minimal fracture length interpreted in the AP3 outcrop (i.e. simulation noise). Consequently all segments smaller than 2.2m where removed from the simulation results. A length frequency distribution was compiled for each of the generated simulations.

The influence of the number of neighbours was evaluated trough 7 simulations (SIM1 to SIM7). The acceptance threshold and the number of neighbours was investigated by comparing 8 simulations (SIM8 to SIM15) where the scanned fraction of the TI was fixed at 25%. The percentage of the scanned fraction of the TI was combined with the 2 other simulation parameters. This combination was tested over 12 simulations (SIM16 to SIM27). The models set-ups and the duration of the simulations are presented in (table 2). Tt is notable that SIM8 / SIM9, SIM10 / SIM11 and SIM13 / SIM14 produce exactly the same network despite the modification of the simulation parameters. Also The MPS algorithm successfully performed SIM16 but the segment extraction generated an error preventing the discretisation of all of the objects~~. No solution was found to solve this issue.~~

The total amount of generated fractures was counted and compared with the total number of fractures interpreted from the original outcrop. A deviation of 10% compared to the original amount of interpreted fractures is considered as a satisfactory result as it is very close to the

reference amount of fractures. A deviation of 20% compared to the original amount of interpreted fractures is considered as an acceptable result. This deviation is consequent but can be adjusted by varying the simulation parameters. A deviation above 20% was rejected as a complete reconsideration of the parameters is required. Results are synthesized in table 3.

The total amount of segments was initially counted in the entire simulation domain. The sum of segments per part is constantly higher than the initial total amount of segments because segments cutting a sharp boundary are divided in two - segments falling within two elementary zones and are consequently counted twice. The number of generated fractures per simulation zone was also computed and the same deviation thresholds were applied to evaluate if the simulation is satisfactory, acceptable or rejected. Tables 4 to 6 synthesize the sensitivity analysis conducted of 27 realisations of the AP3 outcrop.

The length of the segments have been computed for each realisation and are presented in figure 8.

The influence of the hard conditioning data and of the drawing of the training image was also quantitatively investigated and compared respectively with the length of the generated segments and with the amount of segments generated per zone.

- **Summary of the results**

Increasing the number of neighbours rises the computation time (table 2, SIM 1 to 7). A small amount of neighbours results in a noisy simulation (table 2, SIM1). The contrary leads to a downsampling of the generated segments that become longer than the interpreted fractures in AP3 (table 2, SIM7). Decreasing the acceptance threshold leads to an increase of the simulation time (table 2 SIM8-15). Increasing the scanned fraction of the TI is the most time consuming operation (table 2 SIM17-27).

Increasing the number of neighbours only is generally not sufficient to accurately generate a satisfactory or acceptable total amount of fractures (table 3). Increasing the scanned fraction

503 of the TI produces in all cases the closest total number of fractures compared to the reference
504 outcrop (table 3).
505 The counting of fractures in simulation zones revealed that set 2 and set 3 in zone 1, set 3 in
506 zone 4 and set 1 in zone 5 are generally underestimated during the simulation process. In
507 contrast, fracture set 1 in zone 2 is generally overestimated. The consistency of the error over
508 almost the entire set of simulations indicates an issue on the training image representation
509 (table 4-6). Increasing the scanned fraction of the TI generally allows to better represent a low
510 proportion of fracture facies within a TI (Zone TI5, set 2, table 6).
511 An acceptance threshold below 5% leads to an overestimation of the number of small
512 fractures (between 0-10 m), fig 8. In this case, amount of segments between 0-20 m is
513 generally close to the reality. Increasing the scanned fraction of the TI produces the highest
514 quantity of fractures ranging from 0-10 m (fig. 8). Increasing the number of neighbours and
515 the percentage of the scanned TI will result in an increase of the length of the fractures used
516 as hard conditioning data. However, the fracture elongation does not affect all of the hard
517 conditioned fractures and represents a very small percentage of the whole modelled fracture
518 network.
519
520 **III.4.3 Attempt at an optimisation: OPT1**
521 OPT1 was parameterised in regard of the previous observations in order to generate a
522 simulation that is the closest-to-reality possible. For this purpose, the amount of fractures
523 from set 2 and set 3 drawn in TI1 and set 3 drawn in TI4 was increased. In contrast, the
524 amount of fractures from set 1 drawn in TI2 was decreased significantly (fig. 9). We choose
525 to setup the number of neighbours at 50 and the acceptance threshold at 2%. TI1 and TI4 will
526 be scanned at 75% and the rest of the TIs will be scanned at 50% (table 2).

527 The simulation time for the proposed simulation is 2 min 31s (table 2). The total amount of
528 generated fractures is satisfactory compared to the amount of fractures interpreted in the
529 original outcrop.
530 To evaluate the robustness of the optimised simulation, 6 realisations using the same
531 parametrisation were generated for OPT1. The total amount of fractures generated for these
532 simulations always fall below the 10% deviation compared to the reference outcrop.
533 The number of segments comprised between 0-20 m in OPT1 is slightly above the
534 satisfactory deviation limit. As per all the generated simulations, the number of fractures
535 between 2.21 m and 10 m is largely overestimated.
536 OPT1 contains a more satisfactory and acceptable fracture count than any other simulation
537 generated before (table 6). The amount of segments generated in zone 1 and 2 for set 1 is
538 slightly overestimated. In zone 3, OPT1 fails to represent the amount of fractures for set 1
539 (25% deviation) and for set 3. Fracture set 1 in zone 4 is largely overestimated.
540

541 **III.4.4 Evaluation of the AP3 and OPT1 simulations: P21 calculations**

542 Uncertainty analysis is required when performing simulations of geological parameters,
543 especially far from data. The sensitivity analysis presented in this paper is a way to compare
544 the MPS simulations with the reference outcrop.
545 To reinforce the evaluation of the proposed method, we quantified the values of fracture
546 intensity in the reference outcrop, in three selected AP3 MPS simulations and in the optimised
547 simulation (OPT1) (fig. 10). The fracture intensity was classified by (Dershowitz and Herda,
548 1992) in regard of i) the size and dimension (1D, 2D, 3D) of a selected zone of interest and ii)
549 the number, length, area or volume of fractures within this selected zone. In this paper, we
550 chose to calculate the P_{21} fracture intensity, which corresponds to the sum of all fracture

lengths within a regularly discretized spaced, with constant area boxes (10 × 10 m) covering the entire AP3 area of interest.

Visually, the results show an apparent higher P_{21} intensity in the reference outcrop than in the simulations. However, zones of high intensity in the reference outcrop are generally well represented in SIM26 and in OPT1. This is in agreement with the results of the sensitivity analysis showing that SIM26 and OPT1 best represent the number of fractures present in the reference outcrop.

The average fracture intensity in each simulation has also been computed and confirms the observations conducted during the sensitivity analysis. SIM1 and SIM7 present the lowest average fracture intensity (0.095 m^{-1} and 0.079 m^{-1} respectively) and SIM26 and OPT1 present the highest fracture intensity (0.11 m^{-1} and 0.099 m^{-1} respectively). The average fracture intensity in the reference outcrop is higher than in any other simulations (0.126 m^{-1}). However, this value remains close to the ones obtained in SIM26 and OPT1.

The fact that the fractures have been simplified as straight lines in the simulations combined to a relatively small area of calculation (10 × 10 m) could be one element of explanation of the observed fracture intensity variation between the reference outcrop and SIM26 and OPT1. This analysis strengthens the results obtained during the sensitivity analysis and demonstrates the capacity of the MPS method to represent with a high fidelity the geometry of a fracture network.

III.4.5 Using the sensitivity analysis results to model AP4

As per AP3, AP4 present intrinsic an intrinsic variability of the fracture network geometry. This outcrop was divided in 3 elementary zones (fig. 11A-B). According to AP4 partitioning, a probability map with sharp boundaries (fig. 11B) was created. For AP4, the configuration of the outcrop led to mask the area where no interpretation data were performed. In these

576 particular zones a “no data value” was attributed and these masked areas were excluded
577 during the modelling process. In AP4 three training images were created (fig. 11C). As per
578 AP3, the size of the AP4 simulation grid was doubled compared to its original dimension
579 (available in fig.11). In AP4, fractures longer than 40 meters were also considered as hard
580 conditioning data. Here, less than 1.5% of the fractures are longer than 40m (fig. 11D). In
581 AP4, long fractures were found in the 3 sets and mainly in the south-eastern part of the
582 outcrop (fig. 11D, elementary zone 6). 11 N000 fractures (0.5% of the whole), 13 N150
583 fractures (0.6% of the whole) and 9 N090 fractures (0.4% of the whole) were digitized and
584 integrated as conditioning data into the simulation.
585 Based on the results of the sensitivity analysis of AP3 we generated one simulation for the
586 AP4 outcrop (fig. 12). The modelling parameters for SIM AP4-1 were selected as following:
587 the number of neighbours was set up at 50 and the acceptance threshold at 2%. The 3 training
588 images used in the simulation are presented in figure 12 and are considered as representative
589 of the fracture arrangement in each region of the simulation. The scanning percentage of TI6
590 and TI7 was set up at 50%. The scanning percentage of TI8 was set up at 100%. With this
591 configuration, the simulation lasts slightly more than 5 minutes. The fact of intensely
592 scanning TI8 is probably responsible of this duration. The analysis was conducted on the total
593 amount of segments generated and of segments per set of fractures. In AP4 the total number
594 of segments is 1810. The simulation realises 1682 segments in total, which constitutes a
595 satisfactory result. The original AP4 ~~original~~ presents 252 segments striking N150 (set 1), 856
596 segments striking N000 (set 2) and 702 segments striking N090 (set 3). The results of
597 simulation AP4-1 are always satisfactory or acceptable with 206 segments striking N150 (set
598 1), 834 segments striking N000 (set 2) and 642 segments striking N090 (set 3). A detailed
599 analysis was not conducted here because AP4 contains a lot of small fracture intersections

(especially in the TI8 zone) and this makes the segment extraction a complex process. However, these results are promising for the future.

IV] Smooth transitions between elementary zones: towards reservoir scale models to manage uncertainties

The strength of the method proposed here relies on the use of a probability maps and on the opportunity to consider multiple training images in a single realisation to generate non-stationary models of fracture network geometries. In the case of AP3 and AP4, the probability maps are essentially constrained by the variation of geometry of the fracture networks observed on the geological interpretation made on the drone imagery. Consequently, the defined areas are pragmatically bounded and the nature of the limit between one zone and another is a sharp boundary.

AP3 and AP4 outcrops are separated by about 2.5 km and very little is known about the fracture network geometry between these two locations. Assuming that there is no major structural deformation (fold or faults) that may cause a change in fracture geometry at the close vicinity of the outcrop "reality", the zones initially defined on the AP3 and AP4 outcrop can be extended to the limits of the reservoir-scale model boundaries (fig. 13). In this particular case, filling the gap between the two outcrops appears to define how the transition between one side of the simulation grid and the other should be determined.

Fractures are localised objects that do not need to be necessarily continuous from one simulation zone to another. The constant higher proportion of the non-fractured matrix facies versus localised and thin fracture elements ensures the coherency and relative compatibility from one simulation region to another. The idea of the simulation grid region partitioning was re-evaluated and an alternative method, was proposed here. Contrarily to the definition of sharp boundaries in the probability maps used for AP3 and AP4, a probability map with

smooth transitions is defined as follows. An ensemble of elementary zones covering a part of the simulation grid is defined. Each TI corresponds to one elementary zone, which is simulated using exclusively that TI. The probabilities in these zones are then set to one for a specific TI and to zero for the other TIs. The remaining part of the simulation grid is divided in transition zones, for which one has to define which TIs may be involved. In a transition zone, the probabilities of the involved TIs are set proportional to the inverse distance to the corresponding elementary zones. This process creates smooth transitions in low constrained area decreasing the influence of one TI towards another (from one elementary zone to another).

No faults or folds can be initially identified between AP3 and AP4 to condition the drawing of the probability map. In this case, a rectangular compartment representing a gradual probability transition to use the training image associated to one outcrop or to the other filled the blank space between the two outcrops. For instance, fig 13E shows in the Transition_Zone_1 a decreasing probability to use TI1 from left to right (i.e. zone 1 to zone 6) and conversely to use TI6 from right to left.

Recently, investigations conducted on the Rio Grande do Norte geological map (Angelim et al., 2006), demonstrated the presence of a fault crossing the simulation grid near the AP3 zone. This structure may explain the variability of fracture geometry from AP3 (EW stylolites and strong presence of conjugated NS/NW-SE system) to AP4 (EW stylolites associated to NS fracture system, the NW-SE conjugated system is here subordinate). Further geological investigations need to be conducted in this particular place to proof the influence of this fault on the network geometry. However, fig 13F shows an alternative probability map taking into account this interpretation and present how flexible the probability map can be. The proposed method demonstrates its adaptability in various geological contexts.

IV.2 Evaluation of the accuracy of the simulation using mechanical modelling

Uncertainty analysis is required while performing simulations of geological parameters, especially far from input data. The sensitivity analysis presented in this paper is a way to appreciate how good the result provided by the MPS simulation is compared to the reference. However, this test has little meaning when the reference is unknown (e.g. subsurface).

In this case the evaluation of fracture network permeability (i.e. which of the considered fractures are open and are potentially capable to conduct fluid from one point to another) can be tested dynamically and appears to be a good way to validate the provided simulation. This approach can also be extended to fluid flow simulations through the permeable fractures. We calculated mechanical and hydraulic apertures using a Barton-Bandis stress induced aperture model (Barton, 1982; Barton and Bandis, 1980) on the original AP3 interpreted outcrop and on four selected MPS realisations.

Flow in naturally fractured reservoirs is driven by the occurrence of open fractures. The contribution of fractures to fluid flow at in-situ stress conditions in reservoir models can be defined by the Mohr-Coulomb critical stress method (Hoek and Martin, 2014; Rogers, 2003). If shear stress acting on a fracture exceeds normal stress it becomes critically stressed and forms a conduit to flow. The fracture aperture is a key parameters to know for reservoir evaluation and production. The Barton-Bandis empirical model quantifies the aperture that remains when irregular mismatching fracture walls are partially closed under in-situ stress (Fig. 13). The theory and equations behind the use of the Barton-Bandis model are presented in the appendix A of this article.

We chose four MPS generated simulations and the original interpreted fracture dataset for the aperture calculations. We used ABAQUS (Dassault Systemes), a commercial finite element solver for the stress calculations. A conformal mesh consisting of triangular elements is

generated around the fracture traces, which are represented as lower dimensional polyline seams within a 2D plane strain geometry. The number of elements used to mesh the geometries in AP3 original interpreted outcrop is 282020, in SIM1 is 277172, in SIM7 is 272598, in SIM26 is 277778 and in OPT1 is 276702.

An anisotropic load is applied on the four edges of the model to replicate a scenario where the maximum horizontal stress is thrice the minimum horizontal stress in the displacement-loading step. The normal local stress and shear slip, which is heterogeneous, and variable across fracture trace length is hence calculated for the entire fracture system. Longer fractures and intersecting fractures have a larger tendency to slip. Also fractures, which are preferentially aligned to the maximum horizontal stress, would have a greater magnitude of local normal stress. The parameters used for the simulations are tabulated below:

	$Sh_{max} = 30MPa$	$\nu = 0.3\ (-)$	$JRC = 15\ (-)$
	$Sh_{min} = 10MPa$	$E = 35\ GPa$	$JCS = 120MPa$

The resulting aperture distributions can be seen in figure 14. A qualitative comparison of the 5 different DFN's hydraulic aperture distributions demonstrated similar heterogeneities. There are areas within the network, which are open to flow, but also regions, which serve as flow bottlenecks and hence would have a lower permeability. The actual effective permeability of the fractured system under stress would however depend upon the balance between the matrix permeability versus the heterogeneous fracture permeability. Our results indicate that the MPS generated fracture realizations preserve similar regions of open and closed apertures when compared with the deterministic outcrop derived network.

V] A method to create a 3D DFN out of 2D MPS realisations

The MPS simulations presented in this paper are on the form of 2D pixelated maps. MATLAB codes were developed to extract starting and end point coordinates (georeferenced)

699 of a series of aligned colorized pixels that represent a fracture trace from these images.
700 Transforming this output in geologically realistic 3D surfaces is not easy. (Karimpouli et al.,
701 2017) studied samples coming from coalbed methane reservoirs in the fractured Late Permian
702 Bowen Basin in Australia. They realised multiple 2D and pseudo 3D images (i.e. orthogonal
703 2D images) and used the cross-correlation based simulation (CCSIM) to represent the internal
704 organisation of coal cleats and the heterogeneity of the coal matrix in 3D. Their approach
705 greatly improved the understanding of the internal complexity of coal samples and gives
706 better results than classical DFN's based on averaged distributions. However, their method
707 requires an important initial amount of information (i.e. CT scans slices used as training
708 images) that is generally not available at a larger scale. The use of MPS in 3D seems
709 particularly not suited for fracture network representation because: i) they require to associate
710 fractures from 2D map view and from 2D section view (3D or pseudo-3D), ii) it appears
711 difficult to consider isolated fractures in this type of approach and iii) in the subsurface
712 fracture height and/or fracture length are generally unknown.
713 ~~To tackle these problems, we choose to generate statistic fracture networks in 2D map~~
714 ~~environment only~~ To Tackle these problems we choose to use multiple 2D MPS-generated
715 fracture networks. In the presented approach, the 3D is obtained by extruding 3D fracture
716 planes in fracture units (fig. 14). In this approach we consider that fractures are entirely bound
717 to the units, which can appear as a limitation if isolated ~~or aborted~~ fractures occurs inside a
718 layer. However, we can consider variable levels of fracture units. Figure 14 presents an
719 hypothetic scenario where red fractures are confined to a large fracture unit (FU1)
720 crosscutting smaller ones (FU4 containing also smaller red fractures). In such a
721 representation, one 2D planar simulation is required at each top mechanical unit to generate a
722 new set of fractures.

In real-world subsurface configurations, mechanical units can be extracted from well logs (resistivity, density, lithology; (Laubach et al., 2009)). The fracture height distribution, referred as fracture stratigraphy (Hooker et al., 2013) requires here a particular attention and is difficult to extract from borehole data. In outcrops, the use of vertical cliffs adjacent to 2D horizontal pavement should be a way to evaluate these heights and to constrain the 3D model. In outcrops, the resort to vertical cliffs adjacent to 2D horizontal pavements is required to define fracture height. This method is already implemented in gOcad-SKUA software as a macro that extrudes planes of a single fracture family (i.e. all the red fractures in AP3) vertically into a bounded volume (fig. 14). More developments are in process to generate oblique planes and to be able to extrude planes in portions of the fracture ~~family~~ sets.

V] Conclusions

In this paper a new method to predict the geometry of a natural fracture network using the multiple-point statistic algorithm is presented. The method ~~allows to~~ provides stochastic realisation depicting a realistic non-stationary fracture network arrangement in 2D based on the use of multiple, simplified, small training images capturing the natural fracture attributes in specific zones defined by a probability map. Probability maps are adaptable and follow geological rules of fracture type and arrangement distribution specific to various tectonic contexts (i.e. faulting, folding and poor deformation context/no fault, no folds). We developed methods to be able to consider transition zones into the probability maps (e.g. zones far from hard data) that allow simulating fracture network geometry at a larger scale (i.e. reservoir scale).

The realisations obtained from 2D MPS constitute a statistical laboratory close enough to the reality to be tested in terms of fracture mechanical parameters and response to flow. Comparison between mechanical aperture calculation, fluid flow simulations conducted on

both “reality” fracture network interpretations performed on drone imagery and series of MPS realisations gives similar results.

The method proposed here is applicable to all rock types and to a wide range of tectonic contexts. Initially calibrated using outcrop data, the method is fully adaptable to the subsurface in order to better characterise fractures in water, heat or hydrocarbon reservoirs. The challenge there, remains on the definition of the different training images on which the simulation is based. Very few data are generally available in the subsurface and geological rules need to be found to define the geological characteristics of the fracture network (orthogonal or conjugate network) and the associated fracture attributes (length, height, spacing, density, topology).

Acknowledgments

The authors want to thank ENI S.P.A. for the financial support of this research. Silvia Mittempergher from the University of Milano Bicocca is acknowledged for providing the code extracting segments from pixelated images. We would like also to thank the entire SEFRAC group for their interest in developing this method and for their valuable geological advices. Acknowledgements are extended to Philippe Renard from the University of Neuchâtel, to Hadi Hajibeygi from TU Delft and to Wilfried Tsoblefack from Paradigm Geo for the constructive discussions we had together. Prof. Hilario Bezerra from the Universidade Federal do Rio Grande do Norte is acknowledged for providing datasets concerning Apodi area and for his advises on the local geology. We would like to thank Jan Kees Blom from the TU Delft for the improvement he provided to this manuscript.

Appendix A

The DeeSse algorithm (Straubhaar et al., 2011) was used in this paper to reproduce existing fracture network interpreted from outcrop pavements. The following pseudocode developed by (Oriani et al., 2017) have been modified to explain how the algorithm is processing the simulation of fracture. Specific terms can be found in section II.1 of the present paper. In our study the simulation follows a random path into the simulation grid. This grid is step by step populated by values (fracture facies in our case) sampled in the training image. The algorithm proceeds according to the following sequence :

1. Selection of a random location ***x*** in the simulation grid that has not yet been simulated (and not corresponding to conditioning data points, already inserted in the grid).
2. To simulate **V(x)** → the fracture facies into the simulation grid: The pattern $d_n(x) = (x_1,V(x_1)),\ldots,(x_n,V(x_n))$ formed by at most **n** informed nodes the closest to ***x*** is retrieved. If no neighbours is assigned (at the beginning of the simulation), $d_n(x)$ will then be empty: in this case, assign the value **V(y)** of a random location y in the TI to **V(x)**, and repeat the procedure from the beginning.
3. Visit a random location y in the TI and retrieve the corresponding data event $d_n(y)$.
4. Compare ***dn(x)*** to **dn(y)** using a distance **D(*dn(x), dn(y)*)** corresponding to a measure of dissimilarity between the two data events.
5. If **D(*dn(x), dn(y)*)** is smaller than a user-defined acceptance threshold ***T***, the value of **V(y)**is assigned to ***V(x)***. Otherwise step 3 to step 5 are repeated until the value is assigned or an given fraction F of the TI is scanned.
6. if ***F*** is scanned, **V(x)** is defined as V(y), with y the scanned location minimising the distance **D(*dn(x), dn(y)*)**.
7. Repeat the whole procedure until all the simulation grid is informed.

~~Appendix A~~

In the Barton-Bandis stress aperture model, the hydraulic fracture aperture is a function of local stresses, shear displacement, initial roughness of the fracture and mechanical properties of the rock. A set of empirical functions for the mechanical aperture was defined by (Barton, 1982). (Olsson and Barton, 2001) defined the hydraulic aperture as a function of the mechanical aperture. The initial mechanical aperture is given by the following relation from which the mechanical aperture is a function of the Joint Roughness Coefficient (JRC), Joint Compressive Strength (JCS) and uniaxial compressive strength (in MPa).

$$E_0 = \frac{JRC}{5}\left(0.2\frac{\sigma_c}{JCS} - 0.1\right)$$

The JRC is a measure of the relative roughness of the rock fracture surface and is commonly measured using a Barton comb. The JCS can be measured in the field using Schmidt hammer rebound measurements. The joint compressive strength (in MPa) is a mechanical property of the rock. For our simulations, we set JRC = 15 and JCS equal to the uniaxial compressive strength of 120 MPa, so that we obtain an initial unstressed mechanical aperture of 0.3 mm which is independent of length or network geometry. This is valid for an un-weathered fracture where the initial unstressed aperture is only a function of roughness. The mechanical aperture is a function of the normal stress, initial stiffness and the maximum closure.

$$E_n = E_0 - \left(\frac{1}{v_m} + \frac{K_{ni}}{\sigma_n}\right)^{-1}$$

The initial stiffness (in MPa/mm) and maximum closure (in mm) are functions of the JRC, JCS and the initial mechanical aperture.

$$K_{ni} = (-7.15) + 1.75JRC + 0.02\left(\frac{JCS}{E_0}\right)$$

$$v_m = A + B\,(JRC) + C\left(\frac{JCS}{E_0}\right)^D$$

~~The values of the coefficients in the maximum closure equation, vary according to cycles of loading. These coefficients have been given by Asadollahi et al., (2010) and we use the corresponding values for the third cycle where A = -0.1032 ± 0.0680, B = -0.0074 ± 0.0039, C = 1.1350 ± 0.3261 and D = -0.2510 ± 0.1029. The hydraulic aperture, e (in mm) is a function of shear displacement, normal stress, peak shear displacement and mobilized fracture roughness. The shear displacement is obtained numerically. The domain for which $0.75 \leq u_s / u_{peak} \leq 1$ is calculated using linear interpolation (Olsson and Barton, 2001).~~

$$e = \begin{cases} for \dfrac{u_s}{u_{peak}} \leq 0.75 ; \dfrac{E_n^{\,2}}{JRC^{2.5}} \\ for \dfrac{u_s}{u_{peak}} \geq 1; \sqrt{E_n}\, JRC_{mob} \end{cases}$$

~~The peak displacement and mobilized JRC is obtained using the following relations.~~

$$u_{\text{peak}} = 0.0077 L^{0.45} \left(\frac{\sigma_n}{\text{JCS}}\right)^{0.34} \cos\left(\text{JRClog}_{10}\left[\frac{\text{JCS}}{\sigma_n}\right]\right)$$

$$JRC_{mob} = JRC\left[\frac{u_s}{u_{peak}}\right]^{-0.381}$$

~~The peak displacement is a function of JRC, JCS, normal stress and the block size, L (in metres). Within a fracture network, the block size is the spacing of the fracture set intersecting the fracture of interest (Barton, 1982). The mobilized JRC indicates the shear activated fracture wall roughness and is dependent upon the ratio between shear displacement and peak shear displacement.~~

Figure captions

838 **Figure 1:** Direct Sampling method workflow applied to fracture network modelling (modified

839 from (Meerschman et al., 2013).

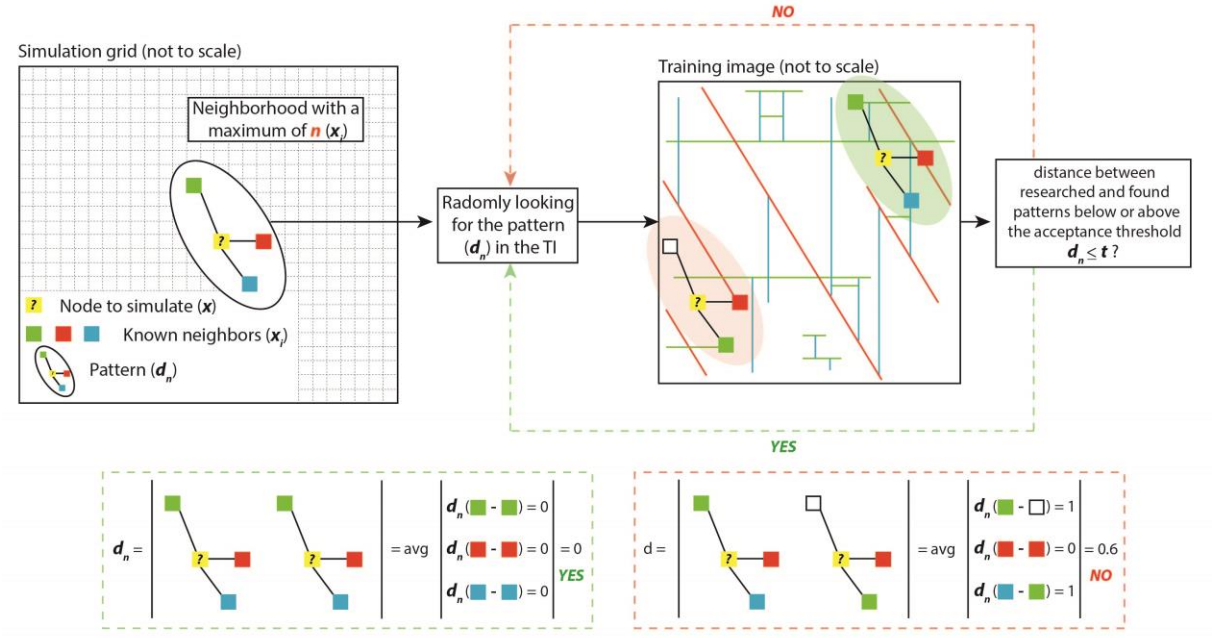

840

841 **Figure 2:** Location of the area of interest and of the studied pavements near Apodi area (red

842 star).

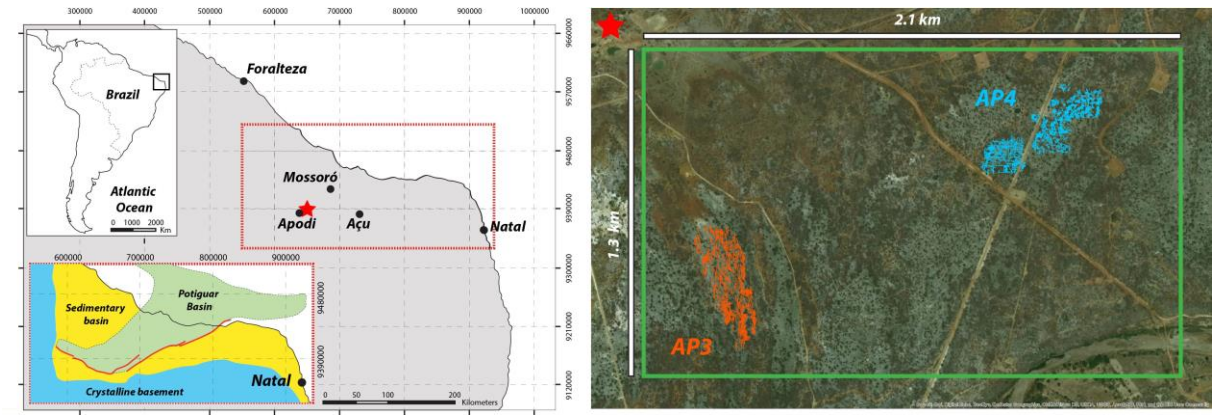

843

844

845

846

Table 1: Outcrop characteristics and fracture parameters collected in AP3 and AP4

AP3 outcrop																			
Localisation (WGS84 UTM Z24S)		*Orientation*	*Dimension*		*Fractures proportion (of the whole fracture population)*														*Fracture length*	
X	Y		NS (m)	EW (m)	Set 1 (N135-N165)					Set 2 (N000-N010/N170-180)					Set3 (N075-N105)					Min (m)	Max (m)
650601	9387908	NNW-SSE	600	300	30%					52%					18%					2,21	123
					Elementary zone 1	Elementary zone 2	Elementary zone 3	Elementary zone 4	Elementary zone 5	Elementary zone 1	Elementary zone 2	Elementary zone 3	Elementary zone 4	Elementary zone 5	Elementary zone 1	Elementary zone 2	Elementary zone 3	Elementary zone 4	Elementary zone 5		
					60%	26%	18%	70%	87%	37%	14%	80%	23%	13%	3%	60%	2%	7%	0%		

AP4 outcrop														
Localisation (WGS84 UTM Z24S)		*Orientation*	*Dimension*		*Fractures proportion (of the whole fracture population)*									*Fracture length*	
X	Y		NS (m)	EW (m)	Set 1 (N135-N165)			Set 2 (N000-N010/N170-180)			Set3 (N075-N105)			Min (m)	Max (m)
652032	9388508	NE-Sw	400	500	20%			40%			40%			1	186
					Elementary zone 6	Elementary zone 7	Elementary zone 8	Elementary zone 6	Elementary zone 7	Elementary zone 8	Elementary zone 6	Elementary zone 7	Elementary zone 8		
					8%	20%	10%	43%	45%	53%	49%	35%	37%		

Figure 3: data acquired in the area of interest in pavements AP3. A) ortho-rectified high-resolution pavement aerial images acquired with a drone, B) fracture interpretation on ortho-rectified images, C) fracture orientation calculated from the north in GIS-based environment. Corresponding rose diagram for both outcrops, D) length of each fracture trace and E) fracture topology relationship for each pavement observed on fracture network interpretation.

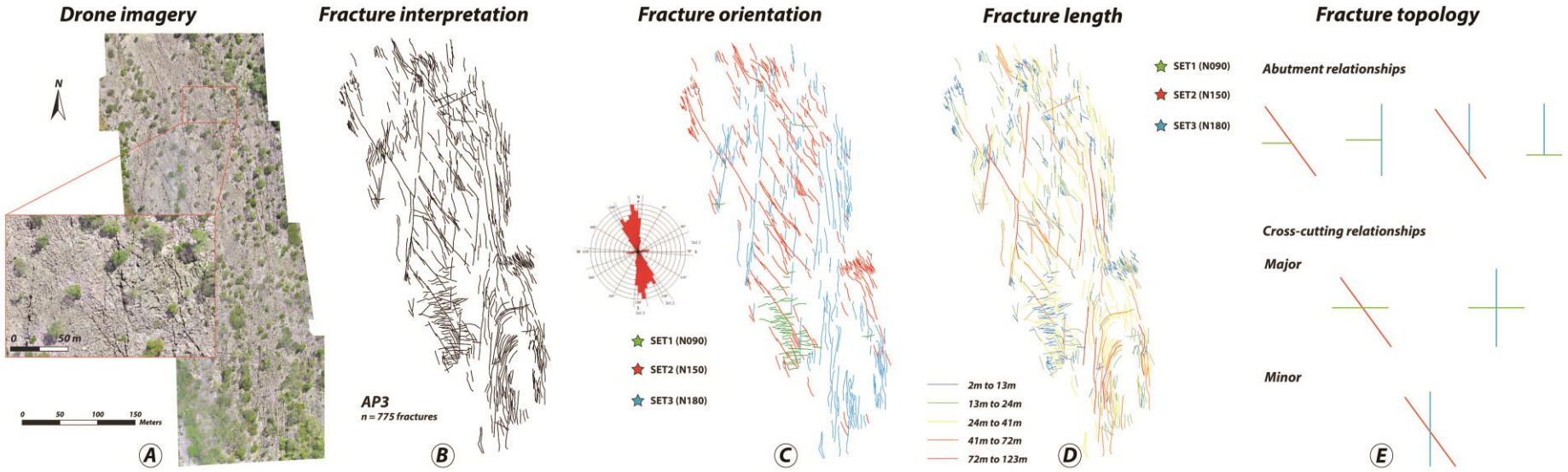

Figure 4: data acquired in the area of interest in pavements AP4. F) ortho-rectified high-resolution pavement aerial images acquired with a drone, G) fracture interpretation on ortho-rectified images, H) fracture orientation calculated from the north in GIS-based environment. Corresponding rose diagram for both outcrops, I) length of each fracture trace and J) fracture topology relationship for each pavement observed on fracture network interpretation

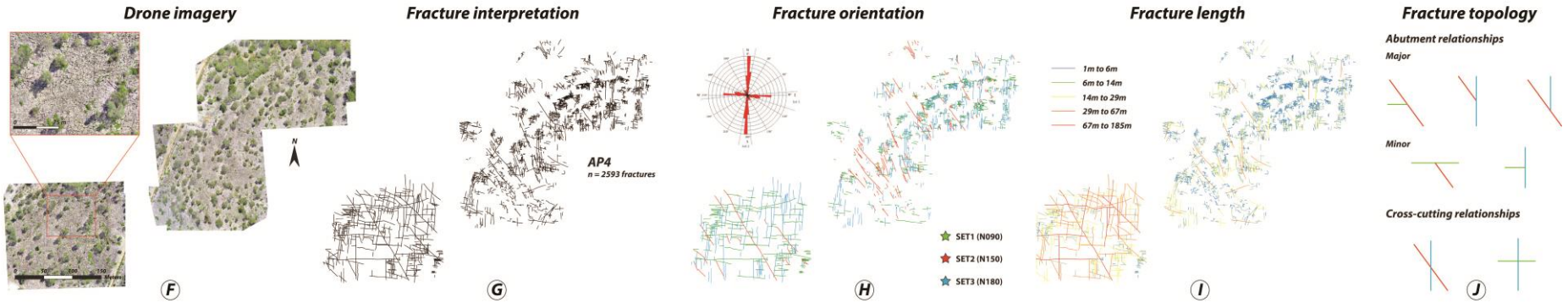

Figure 5: A) Partitioning of AP3 in 5 elementary zones (EZ). This partition is defined (with respect to fracture orientation (fracture facies), fracture density and geometry variability over the entire simulation domain. B) probability map and associated statistics for each EZ. C) training images associated with the partition of AP3. In each EZ, the corresponding training image has a probability (pTI) of 1 to be used. In this zone the other training images are not used (pTI = 0). D) hard conditioning data for AP3. All the fractures longer than 40 m are considered deterministically in the simulation process

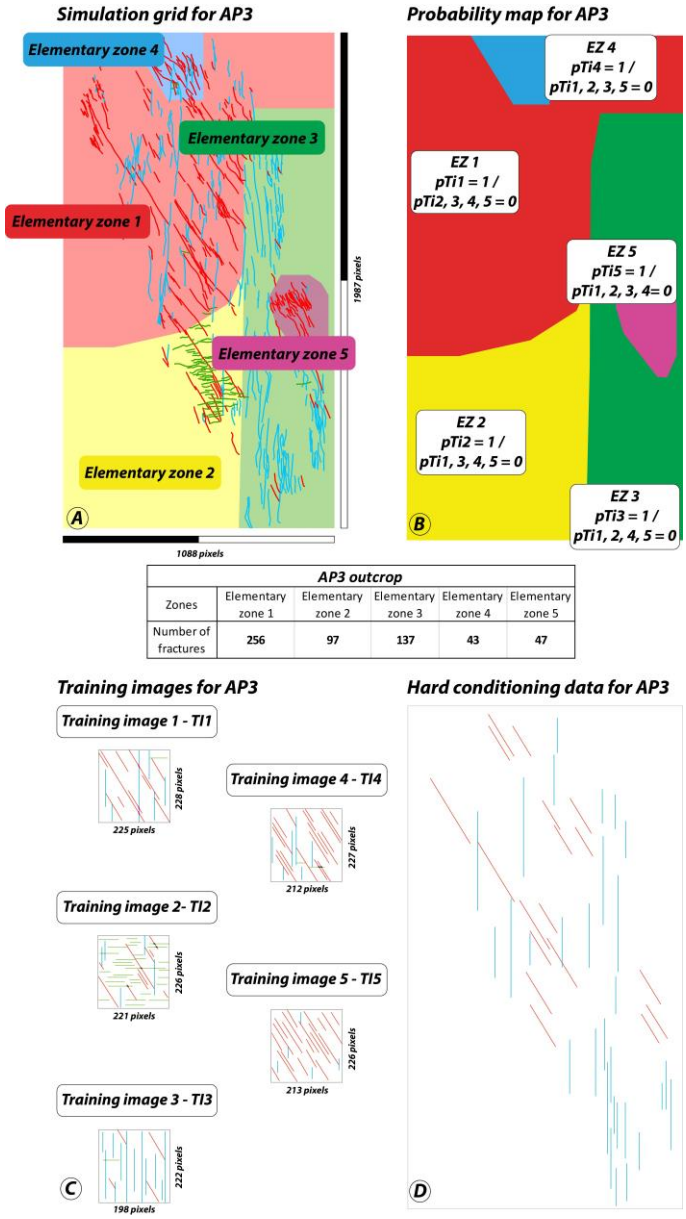

884 **Figure 6:** comparison between results obtained without constraining the topology and with
885 topological facies constraints.

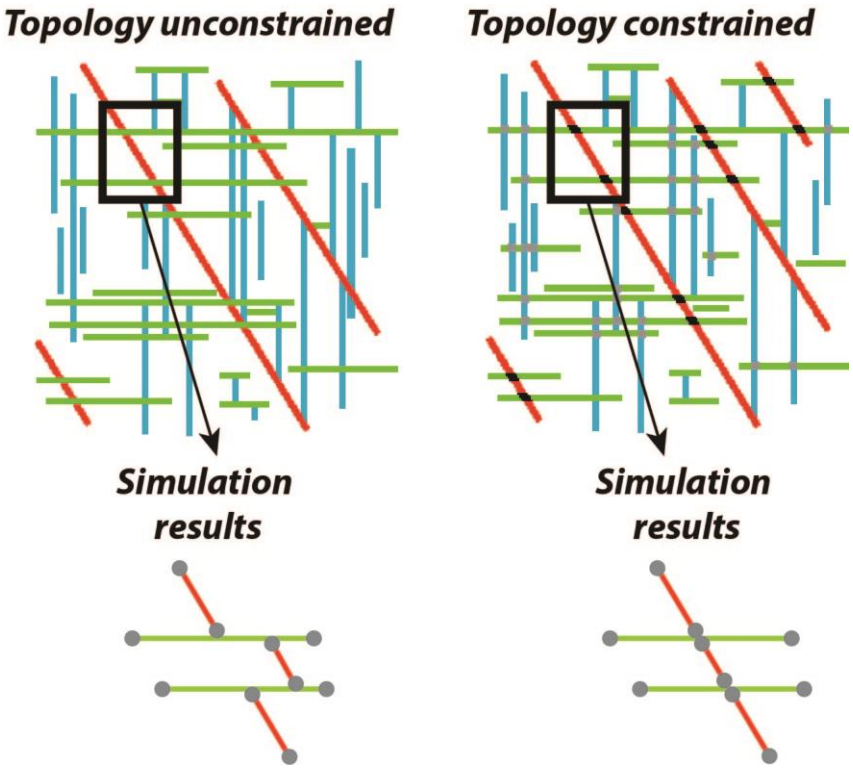

886

887

888 **Figure 7:** visual comparison between: A) the reference fracture network interpretation (AP3),
889 B) the extraction of the longer segments (50 fracture longer than 40m), C) a simulation
890 conditioned by the long segments, D) a simulation not conditioned by the long segments

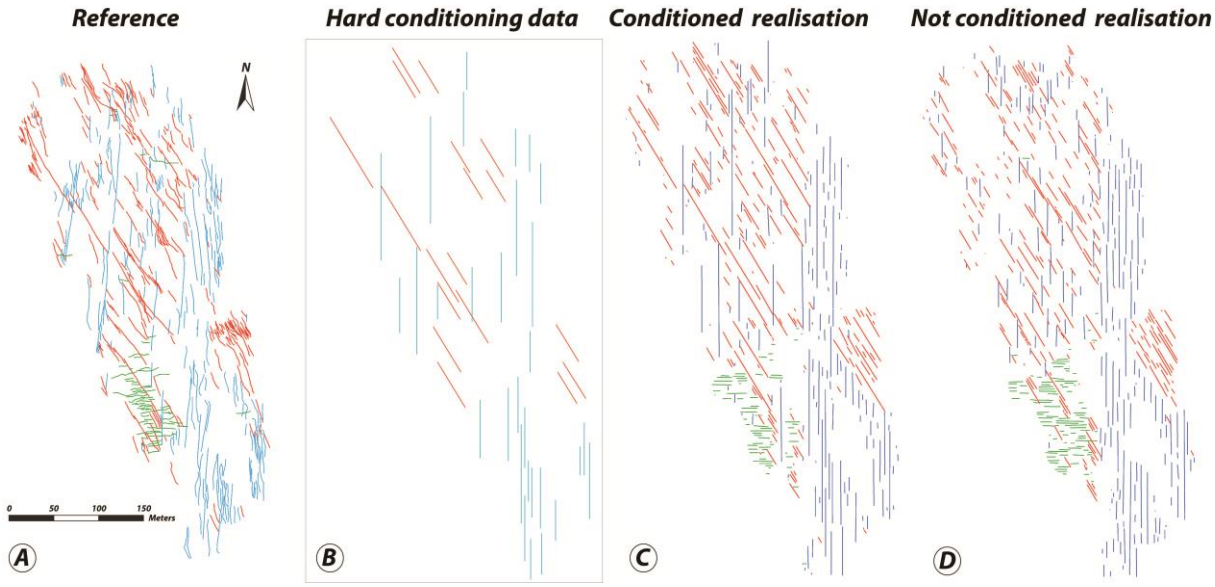

891

Table 2: simulation parametrisation, models set-ups and duration of each run.

Tested parametrisation	*Number of neighbours influence*							*Number of neighbours + Acceptance threshold*							
Realisation name	*SIM1*	*SIM2*	*SIM3*	*SIM4*	*SIM5*	*SIM6*	*SIM7*	*SIM8*	*SIM9*	*SIM10*	*SIM11*	*SIM12*	*SIM13*	*SIM14*	*SIM15*
Simulation parameters	*A. th. = 5% N. = 10 Scan= 25%*	*A. th. = 5% N. = 20 Scan= 25%*	*A. th. = 5% N. = 30 Scan= 25%*	*A. th. = 5% N. = 40 Scan= 25%*	*A. th. = 5% N. = 50 Scan= 25%*	*A. th. = 5% N. = 75 Scan= 25%*	*A. th. = 5% N. = 100 Scan= 25%*	*A. th. = 4% N. = 40 Scan= 25%*	*A. th. = 3% N. = 40 Scan= 25%*	*A. th. = 2% N. = 40 Scan= 25%*	*A. th. = 1% N. = 40 Scan= 25%*	*A. th. = 4% N. = 50 Scan= 25%*	*A. th. = 3% N. = 50 Scan= 25%*	*A. th. = 2% N. = 50 Scan= 25%*	*A. th. = 1% N. = 50 Scan= 25%*
Simulation duration	*22"*	*19"*	*33"*	*36"*	*55"*	*101"*	*136"*	*52"*	*52"*	*90"*	*95"*	*56"*	*76"*	*76"*	*121"*

Tested parametrisation	*Number of neighbours + Acceptance threshold + % TI scan*												*Optimisation*
Group	*Group 1*				*Group 2*				*Group3*				
Realisation name	*SIM16*	*SIM17*	*SIM18*	*SIM19*	*SIM20*	*SIM21*	*SIM22*	*SIM23*	*SIM24*	*SIM25*	*SIM26*	*SIM27*	*OPT1*
Simulation parameters	*A. th. = 3% N. = 40 Scan= 50%*	*A. th. = 2% N. = 40 Scan= 50%*	*A. th. = 3% N. = 50 Scan= 50%*	*A. th. = 2% N. = 50 Scan= 50%*	*A. th. = 3% N. = 40 Scan= 75%*	*A. th. = 2% N. = 40 Scan= 75%*	*A. th. = 3% N. = 50 Scan= 75%*	*A. th. = 2% N. = 50 Scan= 75%*	*A. th. = 3% N. = 40 Scan= 100%*	*A. th. = 2% N. = 40 Scan= 100%*	*A. th. = 3% N. = 50 Scan= 100%*	*A. th. = 2% N. = 50 Scan= 100%*	*Custom*
Simulation duration	*80"*	*148"*	*123"*	*124"*	*105"*	*196"*	*152"*	*154"*	*104"*	*203"*	*150"*	*149"*	*151"*

Table 3: Comparison between the total amount of segments interpreted in the reference outcrop and in the different sets of simulations (tested parametrisation). Evaluation of the results in terms of satisfactory (green symbol), acceptable (orange symbol) or non-satisfactory (red symbol)

				Results evaluation		
	Reference outcrop	*Tested Parametrisation*	*Number of tested configurations*	✔	≈	✘
Total segments	*562*	*Influence of the number of neighbours*	*n=7*	*1*	*1*	*5*
		Number of neighbours + Acceptance threshold	*n=8*	*3*	*2*	*3*
		Number of neighbours + Acceptance threshold + % TI scan	*n=12*	*5*	*6*	*1*

Table 4: results of the sensitivity analysis on the influence of the number of neighbours. The table presents the number of segments per simulation zone for AP3 (used as reference). Red symbols show a total amount of segments of the considered set in the considered zone deviating to more than 20% from the reference case. Yellow symbols show a deviation of more than 10% from the reference case. Green symbols do not deviate significantly from the reference outcrop interpretation.

			Number of neighbours						
		Reference	*SIM1*	*SIM2*	*SIM3*	*SIM4*	*SIM5*	*SIM6*	*SIM7*
		Segments per parts							
Zone TI1	Set1	156	✗	≈	≈	✗	✗	✗	✗
	Set2	95	✗	✗	≈	✗	✗	✗	✗
	Set3	6	✗	✗	✗	✗	✗	✗	✗
Zone TI2	Set1	22	✗	✗	✗	✗	✗	✗	≈
	Set2	12	✗	✗	✓	✗	✗	✗	✗
	Set3	57	✗	≈	✓	✓	✓	≈	✓
Zone TI3	Set1	20	✗	✓	✗	✗	✗	✗	✗
	Set2	113	✗	≈	✓	≈	≈	✗	✗
	Set3	2	✗	✗	✗	≈	≈	✗	✗
Zone TI4	Set1	25	✗	✗	✗	✓	✓	≈	✗
	Set2	10	✓	✓	✓	✓	≈	≈	≈
	Set3	3	✗	✗	✗	✗	✗	✗	≈
Zone TI5	Set1	39	✓	≈	✗	✗	✗	✗	✗
	Set2	2	✗	✗	✗	✗	✓	✓	≈
	Set3	0	✓	✓	✓	✓	✓	✓	✓
		Satisfactory total	*No*	*Yes*	*Yes*	*No*	*No*	*No*	*No*
		# satisfactory	3	3	5	4	4	2	4
		# acceptable	0	4	2	2	3	3	2
		# not acceptable	12	8	8	9	8	10	9

Table 5: results of the sensitivity analysis on the influence of the number of neighbours and of the variation of the acceptance threshold. The colour code is the same as the one used in table 4.

			Number of neighbours + Acceptance threshold							
		Reference	*SIM8*	*SIM9*	*SIM10*	*SIM11*	*SIM12*	*SIM13*	*SIM14*	*SIM15*
			Segments per parts							
Zone TI1	Set1	156	✓	✓	≈	≈	✗	✓	✓	✓
	Set2	95	✗	✗	✗	✗	✗	✗	✗	✗
	Set3	6	✗	✗	✗	✗	✗	✗	✗	✗
Zone TI2	Set1	22	✗	✗	✗	✗	✗	✗	✗	✗
	Set2	12	≈	≈	✓	✓	✗	✗	✗	✗
	Set3	57	✓	✓	✗	✗	✓	✓	✓	≈
Zone TI3	Set1	20	✗	✗	✓	✓	✗	✗	✗	✗
	Set2	113	✓	✓	≈	≈	≈	✓	✓	≈
	Set3	2	≈	≈	✓	✓	≈	✗	✗	✓
Zone TI4	Set1	25	✓	✓	✗	✗	✓	✓	✓	✓
	Set2	10	✗	✗	≈	≈	≈	≈	≈	✓
	Set3	3	✗	✗	✗	✗	✗	✗	✗	✗
Zone TI5	Set1	39	✗	✗	✗	✗	✗	✗	✗	✗
	Set2	2	≈	≈	≈	≈	✓	≈	≈	≈
	Set3	0	✓	✓	✓	✓	✓	✓	✓	✓
		Satisfactory total	*Yes*	*Yes*	*Yes*	*Yes*	*No*	*No*	*No*	*Yes*
		# satisfactory	5	5	4	4	4	5	5	5
		# acceptable	3	3	4	4	6	2	2	3
		# not acceptable	7	7	7	7	9	8	8	7

Table 6: results of the sensitivity analysis on the influence of the number of neighbours, of the variation of the acceptance threshold and of the variation of the percentage of the scanned fraction of the training image. The colour code is the same as the one used in table

			Number of neighbours + Acceptance threshold + % TI scan											*Optimisation*
			Group 1			*Group 2*				*Group3*				
		Reference	*SIM16*	*SIM17*	*SIM18*	*SIM19*	*SIM20*	*SIM21*	*SIM22*	*SIM23*	*SIM24*	*SIM25*	*SIM26*	*SIM27*	*OPT1*
			Segments per parts											
Zone TI1	Set1	156		✓	✓	✓	✓	✗	✓	✓	✓	✗	✓	✓	✗
	Set2	95		✗	✗	✗	✗	≈	✗	✗	✗	≈	✗	✗	✓
	Set3	6		✗	✗	✗	✗	✗	✗	✗	✗	✗	✗	✗	✓
Zone TI2	Set1	22		✗	✗	✗	✗	✗	✗	✗	✗	✗	✗	✗	✗
	Set2	12		✗	✗	✗	✗	✗	✗	✗	✓	✗	✓	✓	✓
	Set3	57		✓	✓	✓	✓	≈	✓	✓	✓	≈	✓	✓	≈
Zone TI3	Set1	20		✗	✗	✗	✓	✗	✗	✗	≈	✗	✓	✓	✗
	Set2	113		✓	✓	✓	≈	✓	✓	✓	✓	✓	≈	≈	✓
	Set3	2		≈	≈	≈	✗	✓	✓	✓	≈	≈	✗	✗	✗
Zone TI4	Set1	25		✗	✗	✗	≈	✗	✓	✓	✗	✗	≈	≈	✗
	Set2	10		✓	✓	✓	≈	✓	✓	✓	✗	≈	✓	✓	✓
	Set3	3		✗	✗	✗	✗	✗	✗	✗	✗	≈	✗	✗	✓
Zone TI5	Set1	39		≈	≈	≈	✗	✗	✗	✗	✓	≈	✗	✗	≈
	Set2	2		≈	≈	≈	✗	✗	✓	✓	≈	≈	✓	✓	✓
	Set3	0		✓	✓	✓	✓	✓	✓	✓	✓	✓	✓	✓	✓
		Satisfactory total		*Yes*	*Yes*	*Yes*	*No*	*No*	*Yes*	*Yes*	*Yes*	*Yes*	*Yes*	*Yes*	*Yes*
		# satisfactory		5	5	5	4	4	8	8	6	2	7	7	8
		# acceptable		3	3	3	3	2	0	0	3	7	2	2	2
		# not acceptable		7	7	7	8	9	7	7	6	6	6	6	5

Figure 8: Fracture length distributions tested during the sensitivity analysis. A) fracture length distribution for SIM1 to SIM7, B) fracture length distribution for SIM10, SIM12, SIM13, SIM15 and C) fracture length distribution for SIM16, SIM17, SIM20, SIM21, SIM22, SIM24, SIM5, SIM26.

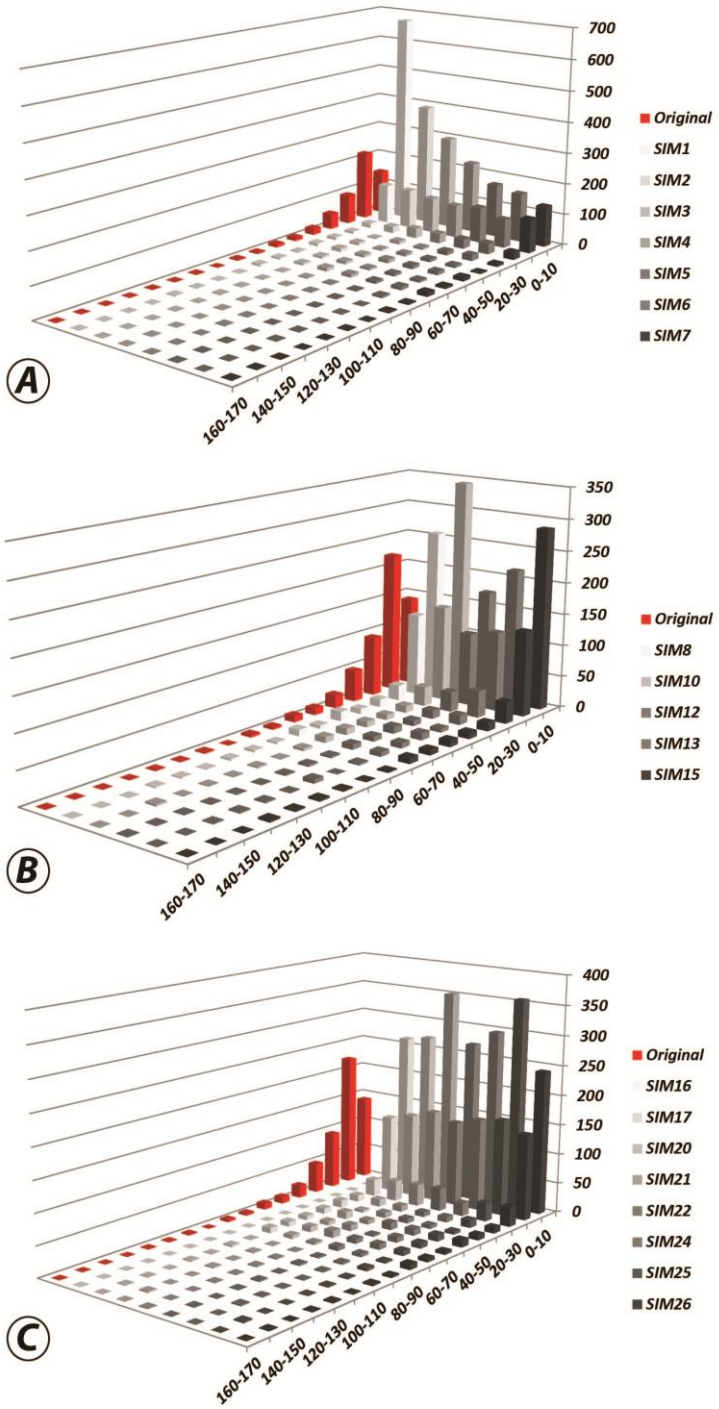

Figure 9: comparison of the training images 1, 3 and 4 used during the sensitivity analysis (27 simulations) and their modification for SIM 3

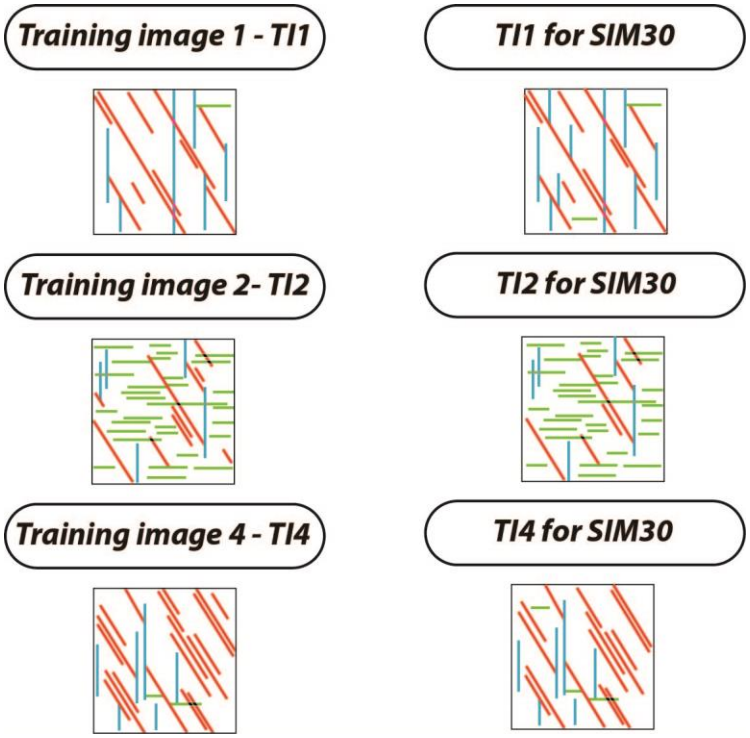

Figure 10: Comparison of the fracture intensity (P_{21}) calculated in the reference outcrop and in four select MPS simulations

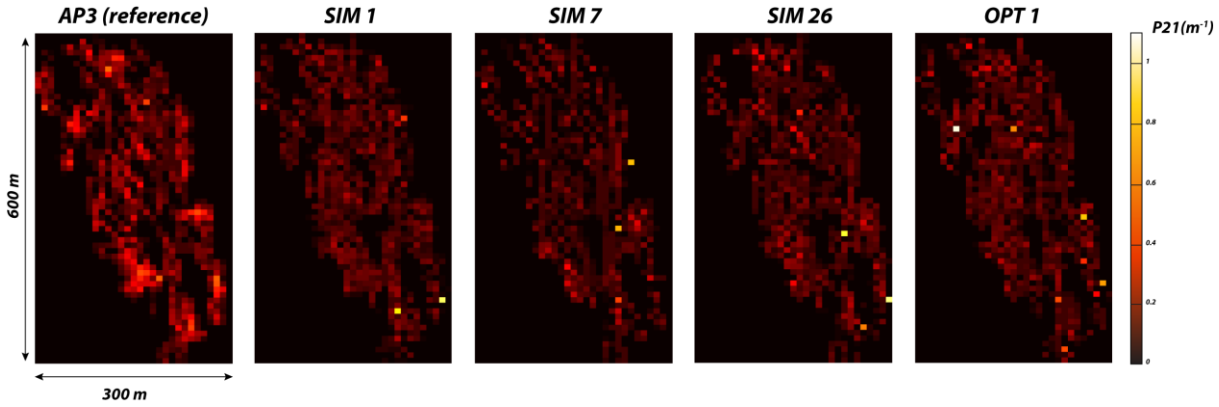

Figure ~~10~~ 11: A) Partitioning of AP4 in 3 EZ. B) probability map and associated statistics for each EZ. C) training images associated with the partition of AP4. D) hard conditioning data for AP4

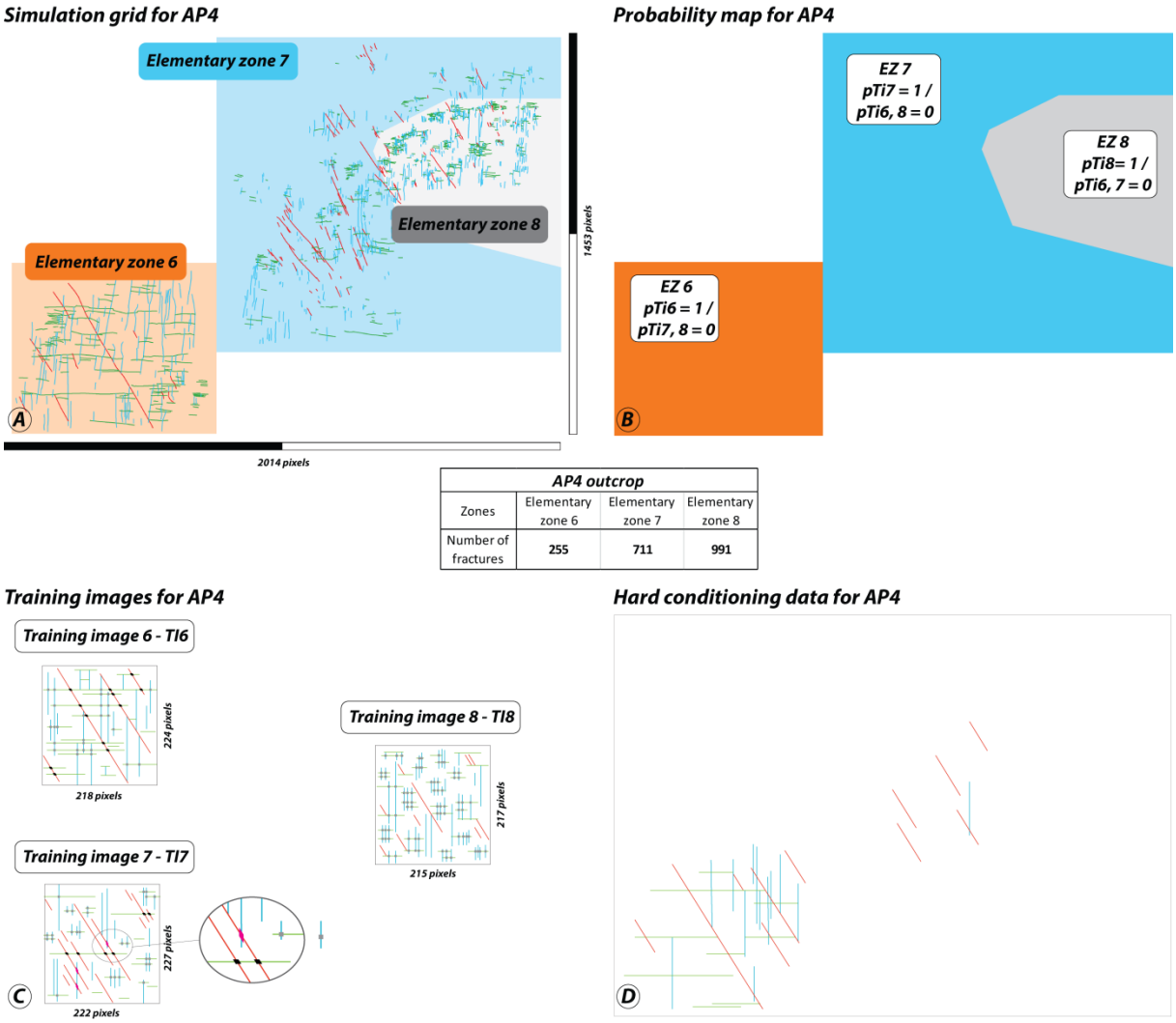

Figure ~~11~~ 12: comparison of the AP4 original outcrop with a MPS simulated version AP4-1

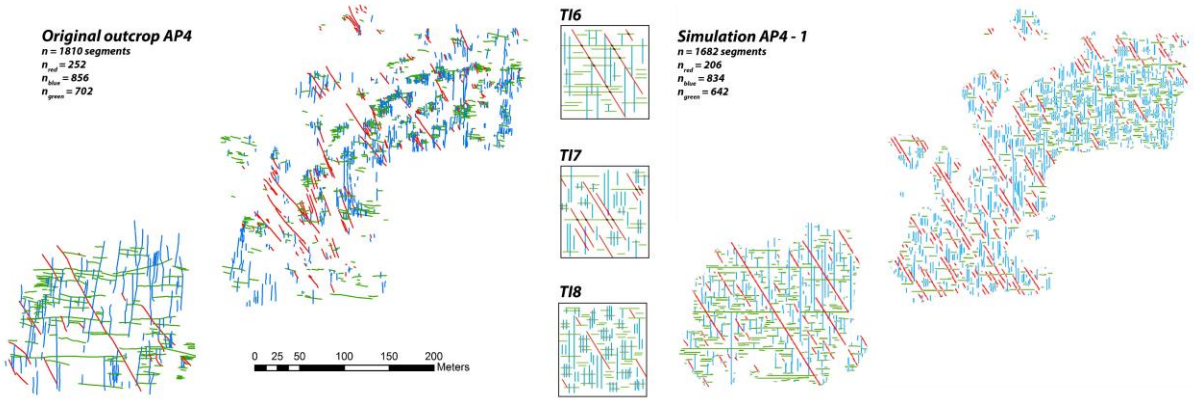

Figure ~~12~~ 13: smooth probability map at the reservoir scale (combination of AP3 and AP4). A) Relative position of AP3 and AP4 outcrops. B) Apodi fault added into the area of interest. Extension of the probability map regions in AP3 and AP4 without geological drivers C) and with the influence of the Apodi fault D). Probability maps with smooth transition zones without geological drivers E) and with the influence of the Apodi fault F).

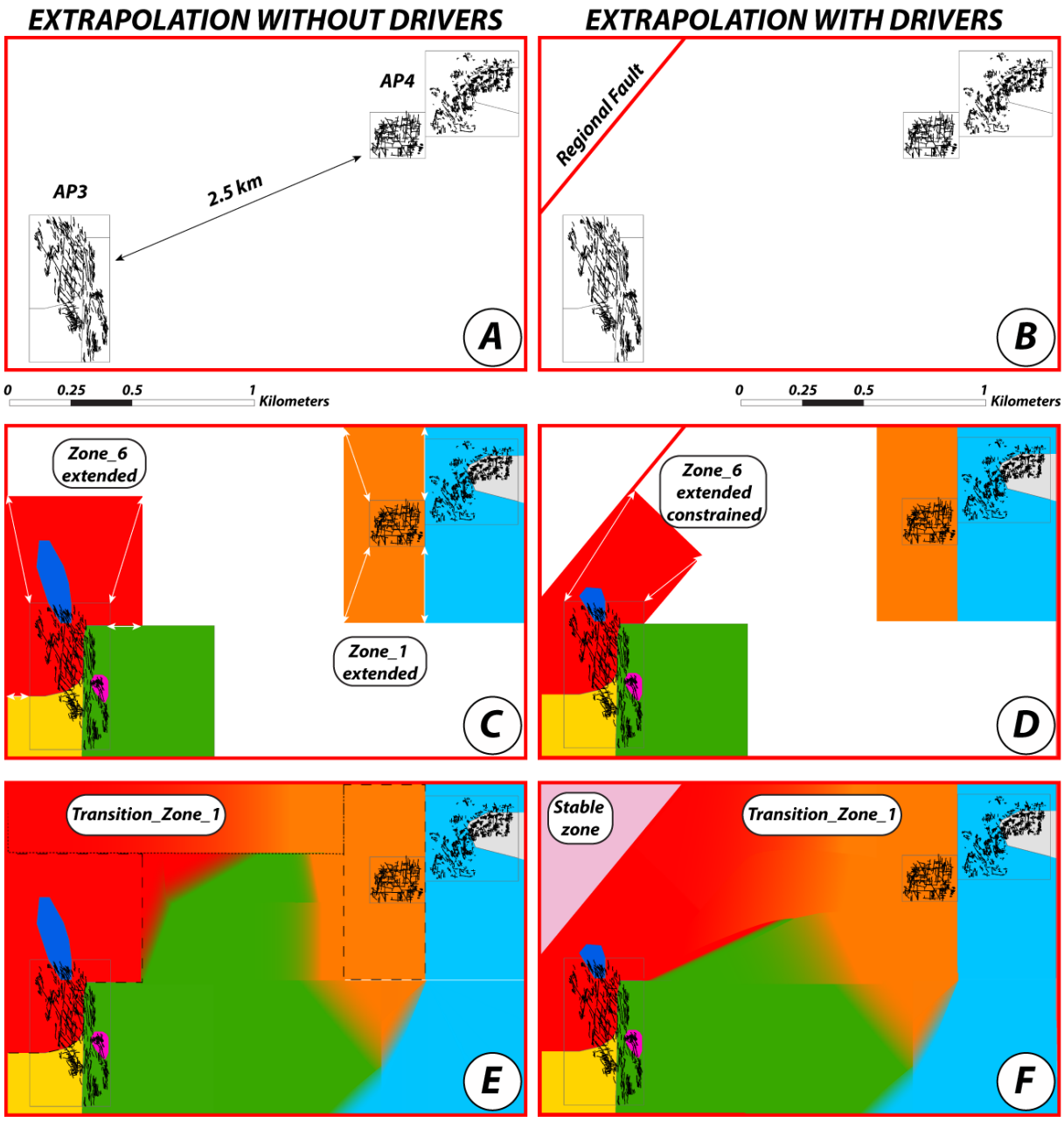

Figure 13: principle and parameters used in the calculation of stress-induced mechanical and hydraulic aperture using the Barton-Bandis approach (modified from (Bisdom, 2016)). The left hand-side sketch represents the initial stage where the fracture is not submitted to stress (aperture is constant). The right hand side sketch represents the same configuration submitted to stress (aperture is not constant).

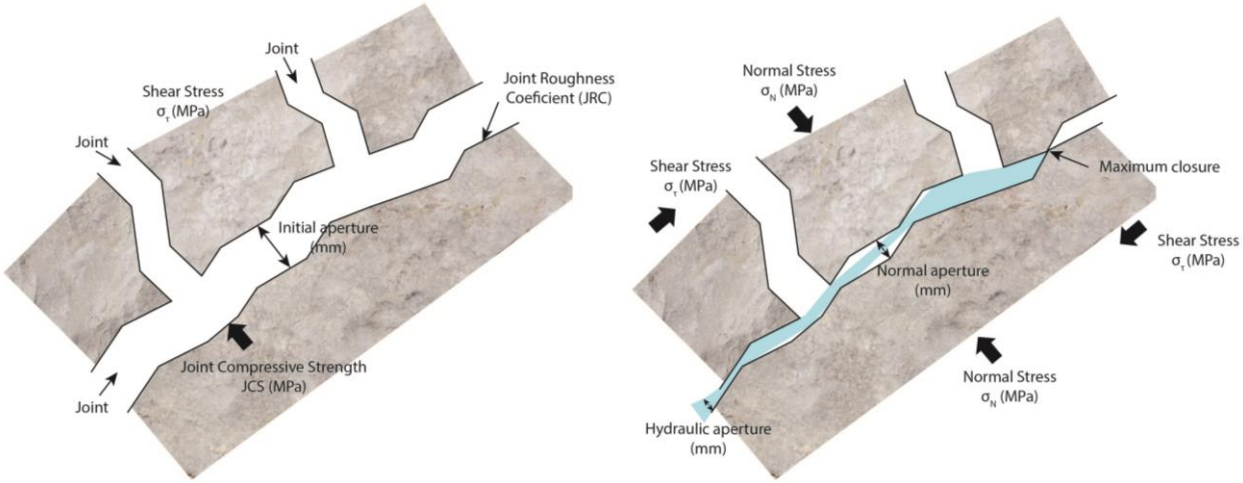

Figure 14: Mechanical and hydraulic aperture calculated in the original outcrop (AP3) and in four selected MPS simulations

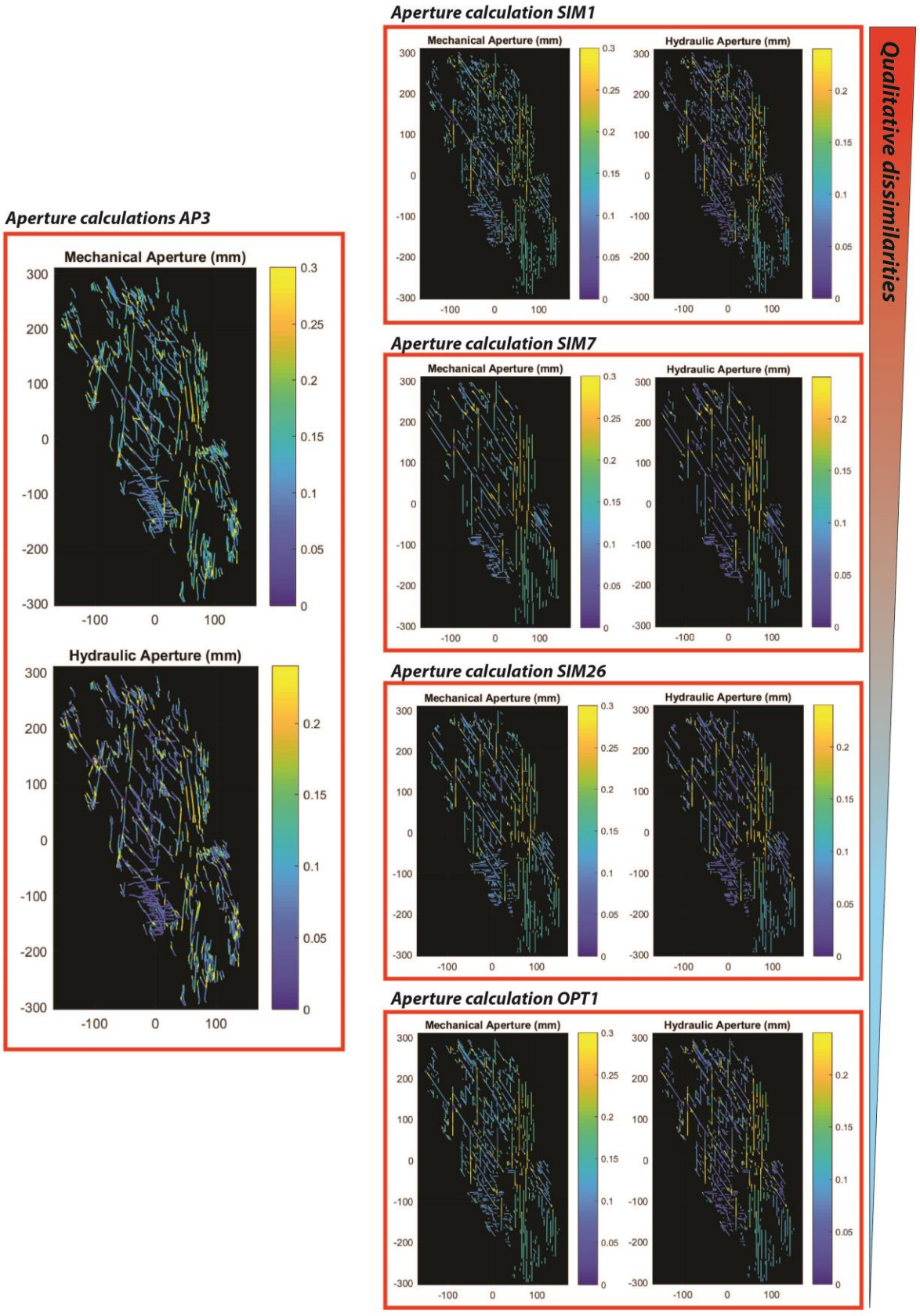

Figure ~~15~~ 14: fracture network extrusion in 3D. The method consists of identifying the different fracture units (FU) on which the fracture height is supposed to be constant (A). This method requires one simulation per top fracture unit (SIM SLICES). (B) is a 3D DFN based on the hypothetical case (A) and realised in gOcad software. (C) is a cross section realised in the centre of the 3D model in the E-W direction.

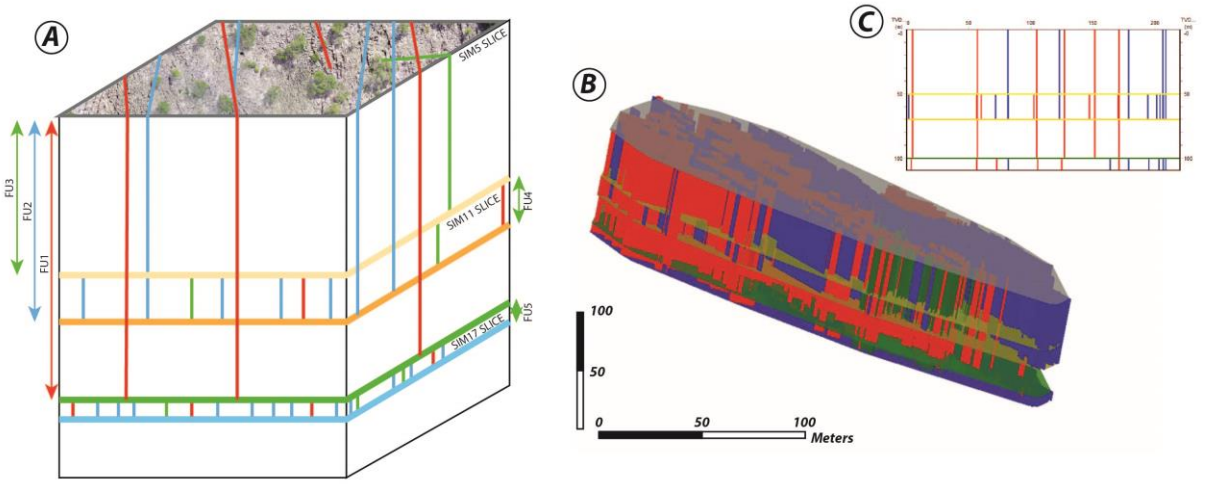

References

Agar, S. M. and Geiger, S.: Fundamental controls on fluid flow in carbonates: current workflows to emerging technologies, Geological Society, London, Special Publications, 406, 60, 2015.

Angelim, L. A. A., Medeiros, V. C., and Nesi, J. R.: Mapa geológico do Estado do Rio Grande do Norte, CPRM/FAPERN, Recife, Projeto Geologia e Recursos Minerais do Estado do Rio Grande do Norte, 2006.

Barton, N.: Modelling rock joint behaviour from in situ block tests: Implications for nuclear waste repository design, Office of Nuclear Waste Isolation, Columbus, OH, USA, 1982.

Barton, N. and Bandis, S.: Some effects of scale on the shear strength of joints, International Journal of Rock Mechanics and Mining Sciences & Geomechanics Abstracts,, 17, 5, 1980.

Bemis, S. P., Micklethwaite, S., Turner, D., James, M. R., Akciz, S., Thiele, S. T., and Bangash, H. A.: Ground-based and UAV-Based photogrammetry: A multi-scale, high-resolution mapping tool for structural geology and paleoseismology, Journal of Structural Geology, 69, 163-178, 2014.

Berkowitz, B.: Characterizing flow and transport in fractured geological media: A review, Advances in Water Resources, 25, 861-884, 2002.

Bertotti, G., de Graaf, S., Bisdom, K., Oskam, B., Vonhof, H. B., Bezerra, F. H. R., Reijmer, J. J. G., and Cazarin, C. L.: Fracturing and fluid-flow during post-rift subsidence in carbonates of the Jandaira Formation,Potiguar Basin,NE Brazil, Basin Research, 29, 18, 2017.

Bisdom, K.: Burial-related fracturing in sub-horizontal and folded reservoirs - Geometry, geomechanics and impact on permeability, Doctorate, Technische Universiteit Delft, 2016.

Bisdom, K., Gauthier, B. D. M., Bertotti, G., and Hardebol, N. J.: Calibrating discrete fracture-network models with a carbonate three-dimensional outcrop fracture network: Implications for naturally fractured reservoir modeling, AAPG Bulletin, 98, 1351-1376, 2014.

Bisdom, K., Nick, H. M., and Bertotti, G.: An integrated workflow for stress and flow modelling using outcrop-derived discrete fracture networks, Computers & Geosciences, 103, 21-35, 2017.

Bruna, P.-O., Guglielmi, Y., Viseur, S., Lamarche, J., and Bildstein, O.: Coupling fracture facies with in-situ permeability measurements to generate stochastic simulations of tight carbonate aquifer properties: Example from the Lower Cretaceous aquifer, Northern Provence, SE France, Journal of Hydrology, 529, Part 3, 737-753, 2015.

Bruna, P.-O., Hardebol, N., Bisdom, K., Straubhaar, J., Mariethoz, G., and Bertotti, G.: 2D to 3D fracture network detection and forecasting in a carbonate reservoir analogue using Multiple Point Statistics (MPS). ExCEL London2017.

Bruna, P.-O., Prabhakaran, R., Bertotti, G., Mittempergher, S., Succo, A., Bistacchi, A., Storti, F., and Meda, M.: Multiscale 3D prediction of fracture network geometry and fluid flow efficiency in folded carbonate reservoir analogues; Case study of the Island of Pag (Croatia). Muscat, Oman, 5-7 February 2018 2018.

Chopra, S. and Marfurt, K. J.: Volumetric curvature attributes for fault/fracture characterization, First Break, 25, 12, 2007.

Chugunova, T., Corpel, V., and Gomez, J.-P.: Explicit fracture network modelling: from multiple point statistics to dynamic simulation, Mathematical Geosciences, 49, 13, 2017.

Claes, H., Degros, M., Soete, J., Claes, S., Kele, S., Mindszenty, A., Török, Á., El Desouky, H., Vanhaecke, F., and Swennen, R.: Geobody architecture, genesis and petrophysical characteristics of the Budakalász travertines, Buda Hills (Hungary), Quaternary International, 437, 107-128, 2017.

1101 Corradetti, A., Tavani, S., Parente, M., Iannace, A., Vinci, F., Pirmez, C., Torrieri, S., Giorgioni,
1102 M., Pignalosa, A., and Mazzoli, S.: Distribution and arrest of vertical through-going joints in a
1103 seismic-scale carbonate platform exposure (Sorrento peninsula, Italy): insights from
1104 integrating field survey and digital outcrop model, Journal of Structural Geology, doi:
1105 https://doi.org/10.1016/j.jsg.2017.09.009, 2017a. 2017a.
1106 Corradetti, A., Tavani, S., Russo, m., Arbues, P. C., and Granado, P.: Quantitative analysisi of
1107 folds by means of orthorectified photogrammetric 3D models: A case study from Mt. Catria,
1108 Northern Apennines, Italy, The photogrammetric record, doi: 10.1111/phor.12212, 2017b.
1109 17, 2017b.
1110 Costa de Melo, A. C., de Castro, D. L., Bezerra, F. H. R., and Bertotti, G.: Rift fault geometry
1111 and evolution in the Cretaceous Potiguar Basin (NE Brazil) based on fault growth models,
1112 Journal of South American Earth Sciences, 71, 96-107, 2016.
1113 Council, N. R.: Rock Fractures and Fluid Flow: Contemporary Understanding and
1114 Applications, The National Academies Press, Washington, DC, 1996.
1115 de Brito Neves, B. B., Fuck, R. A., Cordani, U. G., and Thomaz F°, A.: Influence of basement
1116 structures on the evolution of the major sedimentary basins of Brazil: A case of tectonic
1117 heritage, Journal of Geodynamics, 1, 495-510, 1984.
1118 Dershowitz, W. S. and Herda, H.: Interpretation of Fracture Spacing and Intensity,
1119 Balkema1992.
1120 Deutsch, C. V. and Journel, A. G.: GSLIB : Geostatistical software library and user's guide,
1121 New York, 1997.
1122 Faulkner, D. R., Jackson, C. A. L., Lunn, R. J., Schlische, R. W., Shipton, Z. K., Wibberley, C. A.
1123 J., and Withjack, M. O.: A review of recent developments concerning the structure,
1124 mechanics and fluid flow properties of fault zones, Journal of Structural Geology, 32, 1557-
1125 1575, 2010.
1126 Gringarten, E. and Deutsch, C. V.: Methodology for Variogram Interpretation and Modeling
1127 for Improved Reservoir Characterization, SPE Annual Technical Conference and Exhibition,
1128 Texas, Houston, 1999.
1129 Gringarten, E. and Deutsch, C. V.: Teacher's Aide Variogram Interpretation and modeling,
1130 Mathematical Geology, 33, 507-534, 2001.
1131 Hanke, J. R., Fischer, M. P., and Pollyea, R. M.: Directional semivariogram analysis to identify
1132 and rank controls on the spatial variability of fracture networks, Journal of Structural
1133 Geology, 108, 34-51, 2018.
1134 Hoek, E. and Martin, C. D.: Fracture initiation and propagation in intact rock - A review,
1135 Journal of Rock Mechanics and Geotechnical Engineering, 6, 14, 2014.
1136 Hooker, J. N., Laubach, S. E., and Marrett, R.: Fracture-aperture size—frequency, spatial
1137 distribution, and growth processes in strata-bounded and non-strata-bounded fractures,
1138 Cambrian Mesón Group, NW Argentina, Journal of Structural Geology, 54, 54-71, 2013.
1139 Huang, N., Jiang, Y., Liu, R., and Li, B.: Estimation of permeability of 3-D discrete fracture
1140 networks: An alternative possibility based on trace map analysis, Engineering Geology, 226,
1141 12-19, 2017.
1142 Journel, A. and Zhang, T.: The Necessity of a Multiple-Point Prior Model, Mathematical
1143 Geology, 38, 591-610, 2006.
1144 Journel, A. G.: Beyond Covariance: The Advent of Multiple-Point Geostatistics. In:
1145 Geostatistics Banff 2004, Leuangthong, O. and Deutsch, C. V. (Eds.), Springer Netherlands,
1146 Dordrecht, 2005.

Jung, A., Fenwick, D. H., and Caers, J.: Training image-based scenario modeling of fractured reservoirs for flow uncertainty quantification, Computational Geosciences, 17, 1015-1031, 2013.
Karimpouli, S., Tahmasebi, P., Ramandi, H. L., Mostaghimi, P., and Saadatfar, M.: Stochastic modeling of coal fracture network by direct use of micro-computed tomography images, International Journal of Coal Geology, 179, 153-163, 2017.
Kovesi, P.: MATLAB and Octave Functions for Computer Vision and Image Processing. 2000.
Lamarche, J., Chabani, A., and Gauthier, B. D. M.: Dimensional threshold for fracture linkage and hooking, Journal of Structural Geology, doi: https://doi.org/10.1016/j.jsg.2017.11.016, 2017. 2017.
Lamarche, J., Lavenu, A. P. C., Gauthier, B. D. M., Guglielmi, Y., and Jayet, O.: Relationships between fracture patterns, geodynamics and mechanical stratigraphy in Carbonates (South-East Basin, France), Tectonophysics, 581, 231–245, 2012.
Laubach, S. E., Lamarche, J., Gauthier, B. D. M., Dunne, W. M., and Sanderson, D. J.: Spatial arrangement of faults and opening-mode fractures, Journal of Structural Geology, 108, 2-15, 2018.
Laubach, S. E., Olson, J. E., and Gross, M. R.: Mechanical and fracture stratigraphy, AAPG Bulletin, 93, 1413–1426, 2009.
Lavenu, A. P. C., Lamarche, J., Gallois, A., and Gauthier, B. D. M.: Tectonic versus diagenetic origin of fractures in a naturally fractured carbonate reservoir analog (Nerthe anticline, southeastern France), AAPG Bulletin, 97, 2207-2232, 2013.
Li, J. Z., Laubach, S. E., Gale, J. F. W., and Marrett, R. A.: Quantifying opening-mode fracture spatial organization in horizontal wellbore image logs, core and outcrop: Application to Upper Cretaceous Frontier Formation tight gas sandstones, USA, Journal of Structural Geology, 108, 137-156, 2018.
Liu, X., Srinivasan, S., and Wong, D.: Geological characterization of naturally fractured reservoirs using multiple point geostatistics, 2002.
Liu, X., Zhang, C., Liu, Q., and Birkholzer, J.: Multiple-point statistical prediction on fracture networks at Yucca Mountain, Environmental Geology, 57, 1361-1370, 2009.
Lloyd, S. P.: Least Squares Quantization in PCM, IEEE Transactions on Information Theory, 28, 9, 1982.
Long, J. C. S. and Witherspoon, P. A.: The relationship of the degree of interconnection to permeability in fracture networks, Journal of Geophysical Research, 90, 12, 1985.
Magistroni, C., Meda, M., and Corrao, A.: Faults and fracture network prediction: stress/strain modelling from outcrop analysis to seismic characterisation, Abu Dhabi, UAE, 10-13 November 2014 2014.
Mariethoz, G.: Geological stochastic imaging for aquifer characterization, Doctorate, Faculté des Sciences, Université de Neuchâtel, 229 pp., 2009.
Mariethoz, G., Renard, P., and Straubhaar, J.: The Direct Sampling method to perform multiplepoint geostatistical simulations., Water Resources research, 46, 2010.
Marrett, R., Gale, J. F. W., Gómez, L. A., and Laubach, S. E.: Correlation analysis of fracture arrangement in space, Journal of Structural Geology, 108, 16-33, 2018.
Matonti, C., Lamarche, J., Guglielmi, Y., and Marié, L.: Structural and petrophysical characterization of mixed conduit/seal fault zones in carbonates: Example from the Castellas fault (SE France), Journal of Structural Geology, 39, 103-121, 2012.

Mauldon, M., Dunne, W. M., and Rohrbaugh, M. B. J.: Circular scanlines and circular windows: new tools for characterizing the geometry of fracture traces. , Journal of Structural Geology, 23, 12, 2001.
Meerschman, E., Pirot, G., Mariethoz, G., Straubhaar, J., Van Meirvenne, M., and Renard, P.: A practical guide to performing multiple-point statistical simulations with the Direct Sampling algorithm, Computers & Geosciences, 52, 307-324, 2013.
Micarelli, L., Benedicto, A., and Wibberley, C. A. J.: Structural evolution and permeability of normal fault zones in highly porous carbonate rocks, Journal of Structural Geology, 28, 1214-1227, 2006.
Montanari, D., Minissale, A., Doveri, M., Gola, G., Trumpy, E., Santilano, A., and Manzella, A.: Geothermal resources within carbonate reservoirs in western Sicily (Italy): A review, Earth-Science Reviews, 169, 180-201, 2017.
Olson, J. E., Laubach, S. E., and Lander, R. H.: Natural fracture characterization in tight gas sandstones: Integrating mechanics and diagenesis, AAPG Bulletin, 93, 1535-1549, 2009.
Olsson, R. and Barton, N.: An improved model for hydromechanical coupling during shearing of rock joints, International Journal of Rock Mechanics and Mining Sciences, 38, 13, 2001.
Oriani, F., Ohana-Levi, N., Marra, F., Straubhaar, J., Mariethoz, G., Renard, P., Karnieli, A., and Morin, E.: Simulating Small-Scale Rainfall Fields Conditioned by Weather State and Elevation: A Data-Driven Approach Based on Rainfall Radar Images, Water Resources Research, 53, 8512-8532, 2017.
Otsu, N.: A Threshold Selection Method from Gray-Level Histograms, IEEE Transactions on Systems, Man, and Cybernetics, 9, 5, 1979.
Panza, E., Sessa, E., Agosta, F., and Giorgioni, M.: Discrete Fracture Network modelling of a hydrocarbon-bearing, oblique-slip fault zone: Inferences on fault-controlled fluid storage and migration properties of carbonate fault damage zones, Marine and Petroleum Geology, 89, Part 2, 263-279, 2018.
Reis, Á. F. C., Bezerra, F. H. R., Ferreira, J. M., do Nascimento, A. F., and Lima, C. C.: Stress magnitude and orientation in the Potiguar Basin, Brazil: Implications on faulting style and reactivation, Journal of Geophysical Research: Solid Earth, 118, 5550-5563, 2013.
Rogers, S. F.: Critical stress-related permeability in fractured rocks, Geological Society, London, Special Publications 2009, 10, 2003.
Rzonca, B.: Carbonate aquifers with hydraulically non-active matrix: A case study from Poland, Journal of Hydrology, 355, 202-213, 2008.
Solano, N., Zambrano, L., and Aguilera, R.: Cumulative Gas Production Distribution on the Nikanassin Tight Gas Formation, Alberta and British Columbia, Canada, Trinidad and Tobago Energy Resources Conference, Port of Spain, Trinidad, 26, 2010.
Somasundaram, S., Mund, B., Soni, R., and Sharda, R.: Seismic attribute analysis for fracture detection and porosity prediction: A case study from tight volcanic reservoirs, Barmer Basin, India, The Leading Edge, 36, 7, 2017.
Straubhaar, J., Renard, P., Mariethoz, G., Froidevaux, R., and Besson, O.: An improved parallel multiple-point algorithm using a list approach., Mathematical Geosciences, 43, 24, 2011.
Strebelle, S.: Conditional Simulation of Complex Geological Structures Using Multiple-Point Statistics, Mathematical Geology, 34, 1-21, 2002.
Suppe, J.: Geometry and kinematics of fault-bend folding, American Journal of Science, 283, 73, 1983.

Suppe, J.: Principles of structural geology, Prentice-Hall, Inc., Englewood Cliffs, New Jersey, 1985.
Tavani, S., Corradetti, A., and Billi, A.: High precision analysis of an embryonic extensional fault-related fold using 3D orthorectified virtual outcrops: The viewpoint importance in structural geology, Journal of Structural Geology, 86, 200-210, 2016.
Tavani, S., Storti, F., Lacombe, O., Corradetti, A., Muñoz, J. A., and Mazzoli, S.: A review of deformation pattern templates in foreland basin systems and fold-and-thrust belts: Implications for the state of stress in the frontal regions of thrust wedges, Earth-Science Reviews, 141, 82-104, 2015.
Van Eijk, M.: Analysis of the fracture network in carbonate rocks of the Jandaira Formation in northeast Brazil, 2014. Technische Universiteit Delft, 60 pp., 2014.
Vollgger, S. A. and Cruden, A. R.: Mapping folds and fractures in basement and cover rocks using UAV photogrammetry, Cape Liptrap and Cape Paterson, Victoria, Australia, Journal of Structural Geology, 85, 168-187, 2016.
Wang, S., Huang, Z., Wu, Y.-S., Winterfeld, P. H., and Zerpa, L. E.: A semi-analytical correlation of thermal-hydraulic-mechanical behavior of fractures and its application to modeling reservoir scale cold water injection problems in enhanced geothermal reservoirs, Geothermics, 64, 81-95, 2016.
Watkins, H., Healy, D., Bond, C. E., and Butler, R. W. H.: Implications of heterogeneous fracture distribution on reservoir quality; an analogue from the Torridon Group sandstone, Moine Thrust Belt, NW Scotland, Journal of Structural Geology, doi: https://doi.org/10.1016/j.jsg.2017.06.002, 2017. 2017.
Wu, J., Boucher, A., and Zhang, T.: A SGeMS code for pattern simulation of continuous and categorical variables: FILTERSIM, Computers & Geosciences, 34, 1863-1876, 2008.
Zhang, L., Kang, Q., Chen, L., Yao, J.: Simulation of flow in multi-scale porous media using the lattice boltzmann method on quadtree grids, Communications in Computational Physics 19, 17, 2016.

Dear Reviewer

First let us thank you very much for your comments and for the interest you found in our paper.

In the first paragraph of your review you stated: "this manuscript is designed for a journal like GMD rather than Solid Earth".

As you also mentioned earlier in the review, we believe that the topic is relevant for Solid Earth as it presents an innovative method to build DFN models considering more geology than the existing (exclusively statistical or almost) methods. As stated in the manuscript, we are using an existing algorithm from Mariethoz et al., 2010 that we simply tuned and applied to fracture network geometry predictions. We also think that the paper is quite long and developing the MPS method and the training image further will probably not be really helpful for the reader. We also cited a series of reference papers explaining more in detail how the DS algorithm was written (Mariethoz et al., 2010), how could be used the DS algorithm (Meershmann et al., 2013) and presenting a series of application of MPS to generate fracture networks (Chugunova et al., 2017, Karimpouli et al., 2017, Jung et al., 2013). We believe that these references will greatly help readers to go deeper into the MPS method.

In the manuscript no changes are required

Specific comments

Line 22-33, remove from the abstract, this is material for the intro.

We agree with the reviewer comment and we believe that the initial part of the abstract need to be rephrased . As the same material is stated (differently) into the introduction we did not reintegrated this paragraph there.

In the manuscript, we rewrote line 22 to line 30 from the abstract as following: Natural fractures have a strong impact on flow and storage properties of reservoirs. Their distribution in the subsurface is largely unknown mainly due to their sub-seismic scale and to the scarcity of available data sampling them (borehole). Outcrop can be considered as analogues where natural fracture characteristics can be extracted from high-resolution images acquired from drone and photogrammetry. Outcrops thus become a digital laboratory where the interpreted fracture network can be tested mechanically (fracture aperture, distribution of strain/stress) and dynamically (fluid flow simulations).

Line 30 Avoid citations in the Abstract:

We agree with the reviewer comment

As this line is part of the previously removed paragraph, this comment is already taken into account

Line 34 The abstract should be self-supporting. Define training images:

A training image is a sketch drawn by the user and containing patterns (series of pixels) representing a geological object (e.g. a fluvial channel or a fracture network). In this case, all the statistics generated during the simulation process are not dependent on the simulation algorithm but come from the user-designed training image (Journel., 2003).

Consequently, the realisations should represent a geological concept the user has in mind.
The concept of training image has been fairly well defined in previous studies and we are not sure that this definition will be beneficial to our article.

In the manuscript, we did not extended further the definition of the training image as we thought that the concept is familiar to the major part of the audience of this paper

Line 35 Which process?:

we agree that a process cannot be reproduced by an image. In fact it is a sketch of a network supposed to be representative of the network.

In the manuscript, the term was removed from the manuscript.

Line 38 Same basic concepts of statistic should be expanded:

we understand there that you would like us to define the non-stationarity. As stated in line 93-94: "the local stationarity hypothesis suggests the invariance of all of the generated statistics by translation in the simulated domain". This means for instance that if the user decide that the spacing of fracture family X is 1 m, then each X fracture will be spaced accordingly in the simulation domain. In our case we want to create sub domains, intrinsically stationary but overall inducing variability in the simulation grid. In our case Family X in domain Y (elementary zone) will have a spacing of 1m but family X in domain Z (elementary zone) will have a spacing of 2m.

In the Manuscript the abstract was entirely revised as following
Natural fractures have a strong impact on flow and storage properties of reservoirs. Their distribution in the subsurface is largely unknown mainly due to their sub-seismic scale and to the scarcity of available data sampling them (borehole). Outcrop can be considered as analogues where natural fracture characteristics can be extracted from high-resolution images acquired from drone and photogrammetry. Outcrops thus become a digital laboratory where the interpreted fracture network can be tested mechanically (fracture aperture, distribution of strain/stress) and dynamically (fluid flow simulations). One of those outcrop, a flat pavement from the Apodi area in Brazil, was used as a benchmark to evaluate how good are the Multiple Point Statistics (MPS) to replicate the complex arrangement of a reference manually-interpreted fracture network. The MPS method presented in this article is innovative as it is based on the creation of small and synthetic training images representing the variability of the distribution of fracture parameters observed in the field. These images are flexible as they can be simply sketched by the user. We proposed to use simultaneously a set of training images in specific elementary zones defined in a probability map in order to best represent the non-stationarity of the reference network. A sensitivity analysis emphasizing the influence of the conditioning data, the simulation parameters and the used training images was conducted on the obtained simulations. Fracturing density computations and stress-induced fracture aperture calculations were performed on the best realisations and compared the reference outcrop fracture interpretation to qualitatively evaluate the accuracy of our simulations. The method proposed here is adaptable 5in term of training images and probability map) and introduces geology since the initial part of the simulation process. It can be used on any type of rocks containing natural fractures in any kind of tectonic context. This workflow can also be applied to the subsurface to predict the fracture arrangement and its fluid flow efficiency in water, heat or hydrocarbon reservoirs.

Line 58 determined (instead of inherited):

modification taken into account in the manuscript

Line 97 Explain why fracture connectivity are poorly constrained in these representations:

The fracture network connectivity implies crosscutting or abutting relationship. While scanning the training image, the MPS algorithm is looking for patterns. In this case abutments are easily found, as it is a singular combination of pixel color. However a crosscutting relationship implies that one fracture is above another. Pixel-wise there will be one fracture continuous and another one discontinuous as the crossing locus cannot be the two colors at the same time. Then without considering a particular facies at the crosscutting locus the fact that two fractures are crossing each other is not taken into account and consequently the connectivity is (partially) lost.

In the manuscript we did not explained more as this problem is detailed in line 325-347 and associated with a figure (6)

Section II.1 (The direct sampling methods). This section is extremely difficult to follow

We are aware that this section is difficult to understand as it implies some terms that are very specific to MPS method. However we tried to make a resume of Mariethoz et al., 2010 and others authors that used the same method before us. This part is also very short and we think that it is not mandatory to understand the rest of the paper. We believe however that it is necessary to present this part to audience that is more aware of MPS technique for them to understand on which method we base our calculations.

In the manuscript we decided to not change this part as it is already simplified and must be included into the paper in our sense. However we added in supplementary material a pseudocode of the DS algorithm to help people to better understand how DS is working.

Line 144. Grid in the X&Y axis; what a node does represent?
A node represents a pixel of the grid. A node in the simulation grid is called x, whereas a node in the training image grid is called y. Here “x” and “y” are not related to an axis of the grid.

No change seems to be required in the manuscript

Line 166. Check “Reference”
We apologize for this error into the manuscript. It should have been removed. Indeed it will not appear in the revised manuscript

In the manuscript we removed this error

Section II.3; sub-sub-section “Training images”: this text requires a figure. It is hard to follow it.
We do not believe that a figure of what is a training image should be required. The training image is nothing complex but a simple sketch drawn by the geologist. In the case of fracture network it could also be a photograph with an interpretation on it (representative element area for instance) used to populate one part of the simulation domain.

In the manuscript we will cite figures 5, 6, 9 and 10 where the training images appear to make them more explicit to the reader.

Line 199. This does not make sense. How can an image represent a phenomenon? It is a sketch?

See above the reply concerning line 35

Line 295. How?

We agree that this sentence is out of place

We removed this sentence from the manuscript

Line 312. I suppose that EZ are determined according to their fracture pattern

Yes they are. This is what we meant by visual inspection of the pavement.

We do not think that action is required in the manuscript for this issue

Section IV.2. Is this section really necessary for this work?

The reviewer is probably not fully aware of reservoir simulation grid resolutions and the need for an upscaled value of permeability. One of the purposes of our MPS technique is to generate DFN realizations of which the local response is later upscaled to a field scale reservoir model. For small-scale fracture networks as ours, the fracture aperture is an unknown quantity, which greatly affects the local pressure response. The matter in Section IV.2 discusses a method to calculate this unknown and compare the aperture variability between various MPS realizations. The results of such a geomechanical approach highlight the robustness of the MPS method as it is able to recreate networks that have similar
regions where apertures are open / closed and hence the implications are that they would have a similar fluid flow pressure response.

However following similar comments from the other reviewer we decided to remove this part from the manuscript

Dear Reviewer

First let us thank you very much for the interesting and constructive comments you left on our paper. This letter aims to reply to your specific comments concerning our manuscript

1) This paper presents a specific application of multipoint statistics to generate synthetic non-stationary 2-D DFN models. I don't think that this is the _first_ application of MPS - I seem to remember a number of authors using e.g., SGEMS for generating conditioned fracture fields.

As far as we were aware of we were the first proposing a MPS approach using the Direct Sampling algorithm were multiple training images are used at time in order to predict the geometry of fracture networks in a non-stationary manner. We also developed our own Matlab codes to generate probability maps or to extract segments out of a MPS realisation (image). We are aware about the fact that people in the past tried to model fracture networks using MPS method however they used single training image that should represent the whole variability of the network. After looking specifically for similar work associated to the laboratory developing SGEMs we were unfortunately not able to find any results suggesting that our approach was already tested. If the reviewer can provide specific references we will be very pleased to take them into consideration and to eventually change the title of our article.

We do not think that particular action in the manuscript are required from the reviewer concerning this issue

2) It is greatly appreciated that the paper clearly explains the limitations of the approach, particularly problems in identifying longer fractures. In addition, there are problems in 3D extrapolation, non-planar features, and termination modes.

Thank you for this comment. Indeed we do have some limitations however we are working on methods for solving some of the problems you are mentioning and we hope to be able to release them as publications in the near future.

We do not think that particular action in the manuscript are required from the reviewer concerning this issue

3) In evaluating the generated DFN's, it would be appropriate to quantitatively compare the statistics of generated vs training DFN's in terms of: Intensity spatial distribution as P21 m/mˆ2, orientation distribution for each set, and size (trace length) distribution, and termination modes.

In this paper we made a sensitivity analysis comparing the reference data (fracture tracing made by a geologist on high-resolution drone imagery) with the realisations we obtained. In this part of the work we compared the amount of segments and their length distribution to evaluate if the realisations are good enough or not. We also used a non-standard approach using the Barton-Bandis stress induced aperture calculation to compare some of the best realisations with the reference outcrop.
While, we think that all of those tests are sufficient to show that the approach is giving satisfactory results in this specific case,

We agree to add to our revised manuscript some P21 calculation conducted on the 5 selected realisations presented in figure 14. This part will be inserted just before the section IV on uncertainties

4) I don't understand why the engineering aspects of the project (i.e, using Barton's empirical relationship to define aperture, geomechanical and flow simulations)- are included in the paper. This is a theoretical algorithm paper, not a case study. Perhaps the engineering portions can be put in a separate paper?

Indeed, this attempt of validation of our MPS results is not a conventional way of doing it. However, we strongly believe that calculating fracture aperture has a double interest. Intrinsically the method allows obtaining realistic estimations of fracture apertures in a non-stationary fracture network. These kind of data cannot be obtained directly from observation in the field and getting these data is of primary importance for fluid flow calculations. Secondly, fracture aperture in Apodi outcrops were already calculated by Bisdom et al., 2016, and we wanted to use this work as a base to compare the results of our simulation. By doing so we demonstrated that reference and trained networks behave equally. Indeed they provide similar ranges of apertures and tend to locate open fractures in the same areas. We believe that this approach is an original and interesting way to validate the results of the MPS.

However following similar comments from the other reviewer we decided to remove this part from the manuscript

5) I would appreciate more details on the specifics of the MPS implementation. I don't think that the algorithm could be reproduced by others with just the details provided in the paper. How is MPS used to vary fracture intensity? Trace length? Orientation? How is MPS used to for different sets, or are the sets completely independent models?

As previously mentioned by Journel, 2003 or by Strebelle 2002, the key factor in MPS simulation is the training image used to generate the model. This is why some authors like Hu et al., 2014 use a full reservoir model as training image. In that case all of the heterogeneity is considered and the statistical variability is implicitly generated – among others – during the scanning of the training image. The idea of our paper is to use fracture facies corresponding to the different sets of fractures identified in an entire outcrop – in our case 3 – and to use multiple sketches to vary the parameters you are talking about: the intensity, the length of fracture the crosscutting relationship and more. If you check into figure 5 for instance, you will see that the training images carry a lot of implicit information gathered from field based investigations for instance or from the interpretation of the network from the drone image. The result obtained showed that the algorithm is able to reproduce this variability during the MPS process. We thought that this part is well explained in the "Method" part under "Multiscale fracture attributes" and "Training images, conditioning data and probability map" chapter. However if we do need to rewrite this paragraph we will be pleased to do it on the revised version of our manuscript.

We decided to add a piece of pseudocode in the manuscript as supplementary material to help people to be able to better understand what DS is doing. The following pseudocode is suggested

The DeeSse algorithm (Straubhaar, 2011) was used in this paper to reproduce existing fracture network interpreted from outcrop pavements. The following pseudocode developed by Oriani et al., 2017 have been modified to explains how the algorithm is processing the simulation of fracture. Specific terms can be found in section II.1 of the present paper. In our study the simulation follow a random path into the simulation grid. This grid is step by step populated by pixels y sampled in the training image until

the simulation grid is entirely filled by properties called ***V(x)*** (fracture facies in this case). The algorithm proceeds according to the following sequence

1. Selection of a random location ***x*** in the simulation grid that has not yet been simulated (far from any conditioning data already inserted in the grid)

2. To simulate **V(x)** → the fracture facies into the simulation grid: retrieve a data event $d_n(x)$, corresponding to **n** neighbours around ***x*** thanks to a fixed circular spatial window of radius R. The pattern $d_n(x) = (x_1,V(x_1)),\ldots,(x_n,V(x_n))$ formed by at most **n** informed nodes the closest to ***x*** is retrieved. If no neighbours is assigned (at the beginning of the simulation) and $d_n(x)$ will then be empty: In this case, assign the value **V(y)** of a random location y to **V(x)**, and repeat the procedure from the beginning.

3. Visit a random location y in the TI and retrieve the corresponding data event $d_n(y)$.

4. Compare ***dn(x)*** to **dn(y)** using a distance **D(*dn(x), dn(y))*** corresponding to a measure of dissimilarity between the two data events.

5. If **D(*dn(x), dn(y))*** is smaller than a user-defined acceptance threshold ***T***, the value of **V(y)**is assigned to ***V(x)***. Otherwise step 3 to step 5 are repeated until the value is assigned or an given fraction of the TI, ***F*** is scanned.

6. if ***F*** is scanned, **V(x)** are defined as the scanned datum that minimise the distance **D(*dn(x), dn(y))*** within the simulation grid.

7. Repeat the whole procedure until all the simulation grid is informed.

Dear Stephen Laubach

First let us thank you very much for the very detailed and highly valuable comments you left on our paper. In this letter we tried to reply to all of your comments as precisely as possible. We hope that our answer will satisfy you.

Overall quality: This is potentially a valuable contribution on the topic of understanding fracture networks. Outcrop fracture studies are being revolutionized by the rapid acquisition of fracture patterns from drones and photogrammetry. Developments in statistical approaches to process these observations are needed. This paper makes a credible contribution on the statistical front. And the written presentation and illustrations are fairly clear and compelling. I do think that there is room for improvement to increase the impact of the paper.

Specific comments
C1:In the presentation encompassing figures 3 through 5, I didn't completely follow how you defined 'fracture facies' and 'elementary zones'. Is there some sort of statistical measure of deviation from random you used (as in, for example, Marrett et al. 2018). Or are the 'facies' just qualitatively identified as 'looking similar'? My apologies if I just missed the explanation.

We decided arbitrarily that the facies would be defined in regard of fracture sets (based on orientation). The facies can eventually be made more complex if the user wants for instance to separate different length of fracture within the same set of fracture.
The elementary zones are based on the variability of fracturing intensity per set within the outcrop. This analysis is possible because we have access to the final network that we consider as the "reality". In this case, when we observed a drastic change in the network geometry we placed a boundary around this area and this boundary defines an elementary zone. For instance, EZ1 contains mainly the NS (blue) and the NW-SE (red) fracture sets. On the contrary EZ2 contains mainly EW (green) fractures and EZ3 mainly NS fractures. EZ4 and 5 represent patches where the fracture density is higher. You can see the new density maps in the revised manuscript.

In the manuscript this is explained first in part II.3, probability map. We there the following paragraph
The PM comes from a simple sketch (i.e. a pixelated image) given by the MPS user. It is based on the geological concepts or interpretations that define the geometry variability over the simulated area and that allow a partition of the outcrop. In each of the zones defined into the area of interest, the simulated property will follow the intrinsic stationary hypothesis (citation) but the entire domain will be non-stationary.
While working on outcrops, the partition of the area of interest can be determined based on observations. For instance, when the fracture network interpreted from outcrop images is available, the geologist can visually define where the characteristics of the network are changing (fracture orientation, intensity, length, topology) and draw limits around zones where the network remains the same. This technique was used in the present paper. However, outcrops or subsurface may lack of continuity between observation sites. If the data are sparse and come mainly from fieldwork ground observation or boreholes, the use of alternative statistical approaches can help to provide a robust and accurate partition of the area of interest. The work of Marett et al., (2018) interprets the spatial organisation of fractures using advanced statistic techniques such as normalized correlation count and weighted correlations count, on scanlines collected in the Pennsylvanian Marble Falls Limestone in the United States. In their approach, the periodicity of fracture spacing (clustering) calculated from the

mentioned techniques is evaluated using Monte Carlo quantifying how different from a random organisation are arranged the fractures in the investigated network. These approaches can be highly valuable during the process of building a probability maps when less data are available. The probability maps provide a large-scale….

C2:The abstract reads too much like an Introduction. This part of the text needs to be more information rich. Instead of saying the paper proposes a multiple point statistics method, the Abstract should try to explain the specifics in a highly succinct way. Likewise, how was the method tested; don't just use a passive construction to tell the reader that the method 'was tested'. Bring forward some of the specifics from the Conclusions.

We agree on that point.

In the manuscript, the abstract was modified as following:
Natural fracture network characteristics can be known from high-resolution outcrop images acquired from drone and photogrammetry. These outcrops might also be good analogues of subsurface naturally fractured reservoirs and can be used to make predictions of the fracture geometry and efficiency at depth. However, even when supplementing fractured reservoir models with outcrop data, gaps in that model will remain and fracture network extrapolation methods are required. In this paper we used fracture networks interpreted in two outcrops from the Apodi area in Brazil to present a revised and innovative method of fracture network geometry prediction using the Multiple Point Statistics (MPS) method.
The MPS method presented in this article uses a series of small synthetic training images (TI's) representing the geological variability of fracture parameters observed locally in the field. The TI's contain the statistical characteristics of the network (i.e. orientation, spacing, length/height and topology) and allow representing complex arrangement of fracture networks. These images are flexible as they can be simply sketched by the user.
We proposed to use simultaneously a set of training images in specific elementary zones of the Apodi outcrops defined in a probability map in order to best replicate the non-stationarity of the reference network. A sensitivity analysis was conducted to emphasize the influence of the conditioning data, the simulation parameters and the used training images. Fracture density computations were performed on the best realisations and compared to the reference outcrop fracture interpretation to qualitatively evaluate the accuracy of our simulations. The method proposed here is adaptable in terms of training images and probability map and ensure the geological complexity is accounted for in the simulation process. It can be used on any type of rock containing natural fractures in any kind of tectonic context. This workflow can also be applied to the subsurface to predict the fracture arrangement and fluid flow efficiency in water, heat or hydrocarbon fractured reservoirs.

C3: The introduction could also use improvement. For one thing, the Introduction does not make a very coherent case for why outcrop studies of fractures are so essential. The reason isn't necessarily because fracture networks have 'intrinsic complexity' (line 65) "some networks are quite simple" but because the elements of fracture patterns that govern fluid flow, like connectivity and height and length distribution and the apparent clustered distributions evident in figs 3-5 cannot be adequately sampled in the subsurface. Some attributes like length distribution cannot be sampled at all in the subsurface. Outcrops are where these features can be measured. The Introduction would be stronger if it spelled out this challenge in clear, simple terms.
It would also help if the cited literature included some more explicit examples of how these hard- or impossible-to-measure attributes affect fluid flow (for

example, Long & Witherspoon 1985 on connectivity; Olson et al. 2009 on length distribution in unconnected networks in porous rocks). Right now the Introduction 'lacks motivation'. Many of the parts are there but the case needs to be made stronger. See some of the specific comments below.

We thank you very much for this comment. We will modify the manuscript accordingly.

In the manuscript
Line 65: Despite the existence of these concepts, a range of parameters including fracture abutment relationships as well as height/length distributions cannot be adequately sampled along a 1D borehole and are mainly invisible on seismic images. In addition, fracture networks may present a spatial complexity (variability of orientation or clustering effect) that is also largely unknown in the subsurface. Long and Witherspoon (1985) and Olson et al., (2009) showed how those parameters impact the connectivity of the network and consequently affect fluid flow in the subsurface. In outcrops the fracture network characteristics can be observed and understood directly. Consequently outcrops are essential to characterize fracture network attributes that cannot be sampled in the subsurface, such as length or spatial connectivity.

C4:Ok; the following might seem like a tangential issue. But generalist readers need to have a clear explanation of what problems there might be in using outcrop fracture patterns as analogs for those in the subsurface. In section I.2 about surface rocks as reservoir analogs, an incautious reader would never suspect from the text here that there might be problems with using outcrops fractures for this purpose. This omission needs to be fixed. Some outcrop fractures provide close matches to those in subsurface areas of interest (e.g., Gomez-Rivas et al., 2014) but others do not (e.g., Laubach et al., 2009). In many cases, outcrop fractures provide demonstrably misleading guidance for the subsurface (Corbett et al., 1987 and subsequent work on the Austin Chalk cited in Laubach et al. 2009; Li et al., 2018). Studies typically seek to omit fractures that result from near-surface processes unrelated to fractures at depth (Stearns & Friedman, 1972). But subsurface sampling over the past two decades shows that in the moderate- to deep subsurface (1 km+) in sedimentary basins, many fracture pattern elements differ from those found in more readily sampled outcrops even if the fractures in those outcrops formed in the subsurface, and for unsurprising reasons. Comparative studies in the same rock type and structural setting of fracture spacing observed in outcrop and sampled in long fracture-perpendicular cores shows that patterns in exposures can differ markedly from those in the nearby subsurface (Li et al., 2018, J. Struct. Geol.). The differing temperature-pressure paths of outcrops and rocks at depth and associated differences in rock properties are key reasons that the evidence outcrop patterns provide on fracture patterns in the deeper subsurface needs to be used with caution. The need for caution should be mentioned even if this particular outcrop is a good subsurface analog.
Part of the process of using outcrop fractures is figuring out to what extent the outcrops are guides, and to what circumstances, of the subsurface. This part of the Introduction should acknowledge this issue and mention that the authors addressed it (I notice that later in the MS the outcrops are said to be good analogs; can the authors mention why?). I'm sure the authors recognize this issue and despite the length of my comments a brief but complete acknowledgment of the issue is all that is needed in my opinion.

We will also follow this advice as we are sharing the same opinion on analogues. The issue pointed in the second paragraph of this comment is also approached in the revised text proposed below.

In the manuscript after the line 86 the following text was added
However, not every outcrops can be considered as good analogues for the subsurface. Li et al., (2018), in their work on the Upper Cretaceous Frontier Formation reservoir, USA observed significant differences in the fracture network arrangement in subsurface cores compared to an apparent good surface analogue of the studied reservoir. In the subsurface, fractures appear more clustered than in the outcrop where the arrangement is undistinguishable from random. The origin of these difference is still debated but these authors suggest that alteration (diagenesis) or local change in pressure-temperature conditions, may have conducted to the observed variability. The near-surface alteration processes (exhumation, weathering) may also conduct to misinterpretations of the characteristics of the network. In this case, one should be particularly carful while using observed networks to make geometry or efficiency (porosity, permeability) predictions in the subsurface. Therefore, the application of the characteristics observed in the outcrop to the subsurface is not always straightforward or even possible, and may lead to erroneous interpretations. Relatively unbiased signals such as stylolites or veins and particular geometric patterns might be a trustful basis to show that the studied surface fracture can be, to some extends, compared to the subsurface.

C5:The statistical approach seems like a reasonable one. But I think the paper would benefit from a clearer explanation perhaps aimed at a generalist audience, as well as featuring a compare-and-contrast with other similar approaches. I'd be interested in seeing a comparison with the Hanke et al 2018 directional semivariogram (J. Struct. Geol. 108 [March]).
I noticed that the Liu et al. 2002 citation in your reference list is incomplete. [Liu, X., Srinivasan, S., & Wong, D. (2002, January). Geological characterization of naturally fractured reservoirs using multiple point geostatistics. In SPE/DOE Improved Oil Recovery Symposium. Society of Petroleum Engineers.] If you go to One Petro you can get the doi for papers like this one.

It is true that a lot of work has been done in geostatistics concerning the simulation of fracture network. For instance the work of Bruna et al., (2015 JOH) using two points statistic to evaluate the connectivity of fractured geobodies, the extensive literature using simple or sophisticated DFN (Fracman-type approach) or the approach you mentioned from Hanke et al., 2018 (appearing very interesting). However we believe that MPS is a bit apart in terms of algorithm but also in term of implementation. As we already stated in the new abstract, the goal here is to integrate more geology from scratch (even before starting the simulation) in a series of simple images which are in that respect much more flexible than an average value of density along a well for instance. This is why we did not extend too much on the comparison with other existing methods.

In the manuscript we believe that the new abstract and the part I.3 are sufficient to give to the reader a hint of what are the approaches classically used or used in the past and to present how different and flexible is the MPS approach. However, we added the following paragraph after line 106:
Work of Hanke et al., (2018) uses a directional semivariogram to quantify fracture intensity variability and intersection density. This contribution provides an interesting way to evaluate the outputs of classical DFN approaches but require a large quantity of input data that are not always available in the subsurface. An alternative geologically-constrained method which i) explicitly predict the organisation and the characteristics of multiscale fracture objects, ii) takes into consideration the spatial variability of the

network and iii) requires a limited amount of data to be realised would be an interesting and innovative way to represent fracture network geometry in various contexts.
The second paragraph of the comment was modified in the reference list.

C6:I didn't find the analysis of aperture variation to really be much of a test and the whole exercise seems a bit extraneous to the statistical analysis of the pattern. The text needs to explain more clearly in what sense this is a test (even if that turns out to underline that it is a limited test). As noted below, it would also be appropriate to present the 'stress sensitivity' (or not) of fractures in a more nuanced way. Why no direct measurements of aperture size distributions?

We had similar comments from one of the other reviewer of our paper and we agreed to remove the part talking about fracture aperture IV.2. We admit that the position of this part is not adequately positioned and that the test has a limited impact on the validation of the method already given by a detailed sensitivity analysis. Concerning your last comment we did not took into consideration direct measurements of aperture size distribution for the same reason you mentioned earlier in the review (C4 alteration process). In fact veins are not available everywhere and in each considered sets. This is why the modelling approach appeared to us more robust.

In the manuscript, as already proposed in the answer to one of our Anonymous Reviewer we will add a small visual comparison of the P21 between the 5 models proposed in the figure 14. This part will be added as a III.5 before the discussion.

Technical questions & comments
C7:30 Abstracts do not normally contain citations.

The citation will be removed

In the manuscript the new abstract will not contain citations.

C8:53 'Ubiquitous' means that fractures are everywhere but excavations and horizontal core studies show that some rocks in the subsurface lack fractures, or if fractures are present they are so widely spaced (hundreds of meters or more) that 'everywhere' is not an apt description. An outcrop example showing how resistant to fracture some rocks are is Ellis et al. 2012, J. Geol. Soc. London. A better word might be 'widespread'. Moreover, areas of completely sealed fractures are also common in the subsurface, and such fractures are rarely fluid conduits. Although I don't agree with people who don't count such rocks as fractured, it's certainly the case that some rocks lack fracture flow conduits.

We understand this comment and we will modify the phasing in the manuscript.

In the manuscript the sentence will be modified as following: Fracture are widespread in Nature and depending on their density and their aperture, they might have a strong impact on fluid flow and fluid storage in….

C9:55 I think more caution is called for in citing for this point (effects of fractures on fluid flow). There are relatively few papers that document the effects of fractures on fluid flow in hydrocarbon reservoirs but many papers that repeat the contention that fractures are important for fluid flow. One of the papers that does quantify production data with respect to natural fractures is Solano et al, 2011

SPE Reservoir Evaluation & Engineering. However, although both of the papers cited here in the MS are interesting contributions, I don't think they are the right papers to cite in support of the point the authors make. All of the references mentioned in his section of the text should be reviewed with this point in mind.

We think that the authors cited in this section are all dealing with fractures affecting subsurface reservoirs or surface reservoir-analogues in different contexts and they all seem to converge on the conclusion that fracture play a role (positive or negative) in fluid flow. We agree however that the paper from Solano deserves to be cited there in addition to the Agar and Geiger and Lamarche et al.

In the Manuscript the reference was added in line 55

C10:58-ca. 62 Ok, so maybe a quibble, but 'well known'? really? Maybe I'm not following what the authors are trying to say here, but connecting the specific strain and stress conditions to the formation of a given fracture or fracture pattern is full of uncertainty: the timing of fracture formation is commonly very challenging to estimate unambiguously and because fracture arrays are generally low strain phenomena and through geologic time a wide range of loading paths might lead to fracture (e.g., Engelder 1985, J. Struct. Geol.) the connection between pattern and cause is frequently ambiguous. A good example relevant to this paper is fractures in outcrop. Did they form due to some process at depth (for example, elevated pore fluid pressure) or during uplift or exposure? This issue gets to the reliability of outcrop-derived fracture pattern information (which I'm all in favor of obtaining) but the challenge of determining the causes of fractures I think needs a bit more thoughtful or nuanced treatment.

We admit that a strong shortcut has been made there and that the phrasing has to be revised. In our case fractures form in the response of loading. The differences in patterns between two outcrops AP3 and AP4 distant of about 2.5 kilometres are still debated. However Bertotti et al., 2017 bring some new answer to those questions.

In the manuscript the lines 58-62 have been removed and replaced by: These conditions have been used to derive concepts of fracture arrangements in various tectonic contexts and introduced the notion of geological fracture-drivers (fault, fold, burial, facies). Based on these drivers it is possible to some extents to predict reservoir heterogeneity…

C12:67 Do you mean stresses in the past when fracture patterns formed (paleo stresses)? You seem to be claiming that fractures are highly sensitive to current stress state. I know this is a widely accepted premise, but you should at least note that many reservoirs are known to have fractures that are stiff and insensitive to current stress state (e.g., Laubach et al., 2004, Earth & Planetary Science letters).

We were there talking about paleostress. However, this paragraph was modified according to the comment you made earlier.

In the manuscript: see the response provided in C3

C13: 71-86 This section needs to contain some caveats about the limitations of outcrop fracture research.

This issue was addressed in the general comments mentioned before and have been modified in the manuscript.

In the manuscript: see the response provided in C3

C14: 73 The use of outcrop fracture patterns to constrain the subsurface goes much deeper into the past than the recent references cited here: National Research Council 1996. Rock fractures and fluid flow: Contemporary understanding and applications. National Academy Press, Washington D.C., 551 p.

We agree that this reference is important and we will follow the advice of the reviewer without removing most recent citations.

In the manuscript: the reference was added

C15:81-82 The 'how, when, and where' is rarely obvious from the pattern alone. Flagging this comment is not off topic since it relates to how outcrop data can or should be used.

This was the goal of this sentence. A lot of interpretations is possible from collected outcrop data. This is why we put the word eventually in this sentence. We do not see specially what the reviewer means there.

In the manuscript we did not changed this sentence.

C16:89 'provide'

Changed

In the manuscript we modified "are providing" with "provide"

C17:93-94 This sounds like jargon; provide a clearer explanation of what you mean for a general audience.

We modified the text

In the manuscript the sentence was separated in two parts:
The generated models follow a local stationarity hypothesis. This implies that the statistics used during the simulation are constant in the defined area of interest….

C18:113-119 This is too late in the MS to introduce this material. Some of this could be in the Abstract.

We agreed on that and we changed the abstract as per the answer to comment C2

In the manuscript the abstract was changed

C19:125 What do you mean by 'full outcrops'. This seems vague. If you have a size range in mind, why not state it?

We were working on outcrops which sizes are in the order of 100m. The exact dimension of these outcrops is presented in table1.

In the manuscript the sentence was modified as following:
"…geometry variability over outcrops (size order of 10^2m) and a methodology."

C20:135 I'm not sure I follow you here. You didn't measure any apertures in outcrop, did you? So is this just a process of a computation applied to both the outcrop imaged fractures and the statistical realizations? Why no measured outcrop apertures?

Some apertures were measured in outcrops but we did not used them in this work as we favoured the modelling part. We did not took into consideration surface fracture apertures because they were not representative of the subsurface conditions (weathering issues and exhumations). In any case the part on fracture aperture will be removed from the manuscript.

In the manuscript the sentence: "we computed mechanical and hydraulic apertures in outcrop fracture interpretation and on the obtained stochastic models." Was removed and replaced by "we computed density maps in outcrop fracture interpretation and on selected stochastic models."

C21:205-206 Some of the text here sounds like it is carry over from a proposal, since you've done the work.

We will remove "propose to" from the manuscript

In the manuscript we replaced it by "we used multiple training image"

C22:271 Does the karst figure into your aperture calculations?

Unfortunately not. But we believe that the karstification is due to "recent" surface alteration and will not be present in the subsurface as we can see them today in the outcrop. This topic is close to the one discussed in C4.

In the manuscript: no change applied except that the part on aperture was removed.

C23:322 This seems late in the text to have this kind of preview of goals?

We agree that this sentence is out of place

In the manuscript we removed line 332 to 324.

C24:365 Interesting. Are some of the >40-m-long fractures still censored by outcrop size?

Yes few of these fractures are censored by the boundaries of the outcrop. However a large majority of the fracture are included inside the pavement and we assume that they are representative of the maximal length of the fractures there.

No changes were requested in the manuscript

C25:572-575 There are some jumps in logic here. Yes, flow depends on open fractures. But whether or not fractures are open or not does not simply depend on in situ stress conditions. Some (many) fractures are insensitive to stress state (they are very stiff) and some are closed because they are mineral filled. It therefore does not necessarily follow that 'contribution of fractures to fluid flow: : :can be defined by the Mohr-Coulomb: : :' etc. The development here needs to be more nuanced and include a few caveats. It is also worth noting I think that the predominant role of aperture in fluid flow presumes a completely impermeable

host rock, which is generally not a good assumption even for low porosity unconventional reservoirs (TGS; shale). If there is flow in the host rock and the fractures are not interconnected, open length distribution is what matters (Philip et al. 2005). Philip et al. varied the apertures in their simulations by a lot and got no significant difference in flow. Philip, Z. G., et al., 2005, Modelling coupled fracture-matrix
fluid flow in geomechanically simulated fracture networks: SPE Reservoir Evaluation &
Engineering, 8/4, 300-309.

Thank you for this comment and for the interesting reference you provided. However as this part was removed from the paper this matter will (hopefully) be addressed in a separate paper.

In the manuscript part IV.2 was removed

C26:576 'a key parameter'; if it's a key parameter, why were apertures not measured in the field?

As discussed previously we wanted to apply the aperture calculation into subsurface conditions so we did not considered fracture aperture measured in the field.

In the manuscript part IV.2 was removed

C27:622 'statistic'; is this the word you mean? Obscure usage.

We agree on this comment

In the manuscript the sentence was replaced by: "To Tackle these problems we choose to use multiple 2D MPS-generated fracture networks".

C28:625 What do you mean by 'aborted' fractures? Non-standard usage; suggest you pick another word.

We agree on this comment

In the manuscript the word aborted was removed

C29:632 Mechanical stratigraphy is readily measured in the subsurface; 'fracture stratigraphy' is more challenging. Did you rigorously describe your fracture height patterns for the outcrops (maybe it is in one of the cited references). Height patterns and fracture stratigraphies have different patterns. There is a useful classification in Hooker et al. 2013, J. Struct. Geol.

In fact the aim of this part was to provide a way to use 2D MPS in 3D. We showed our idea and we built a very simple 3D DFN based on our outcrop. The method is now much more elaborated and takes into consideration the issue you mention**.**

In the manuscript we had the following sentence after the Laubach et al., 2009 citation: The fracture height distribution, refered as fracture stratigraphy (Hooker et al., 2013) requires here a particular attention and is difficult to extract from borehole data. In outcrops, the use of vertical cliffs adjacent to 2D horizontal pavement should be a way to evaluate these height and to constrain the 3D model.

C30:637 'fracture family' is non-standard usage. Is there a reason not to call these groupings 'fracture sets' (Hancock, 1985)?

We agree on this comment

In the manuscript fracture family was replaced by fracture sets

C31:641 'provides'; ('The method provides a realistic: : :')

We agree on this comment

In the manuscript the suggested sentence was inserted

C32:Fig. 8, caption 'Fracture: : :'

We agree on this comment

In the manuscript fracture will appears with a capital "F" there

C33:Fig. 10. Some of the colours on this figure make it hard to read.

We agree on this comment

The figure was modified for the article

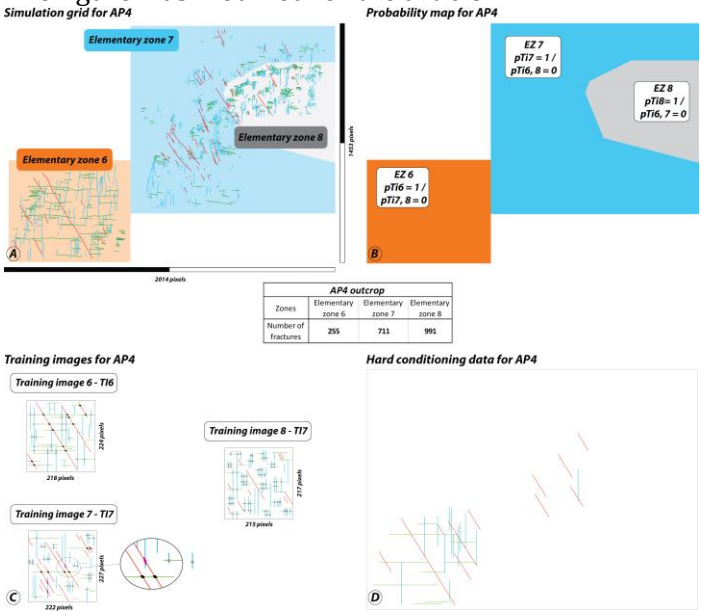

C34:Fig. 12 would be more informative with more labelling and explanation on the face of the figure. Add a graphic explanation/key.

We agree on this comment

The figure was modified for the article

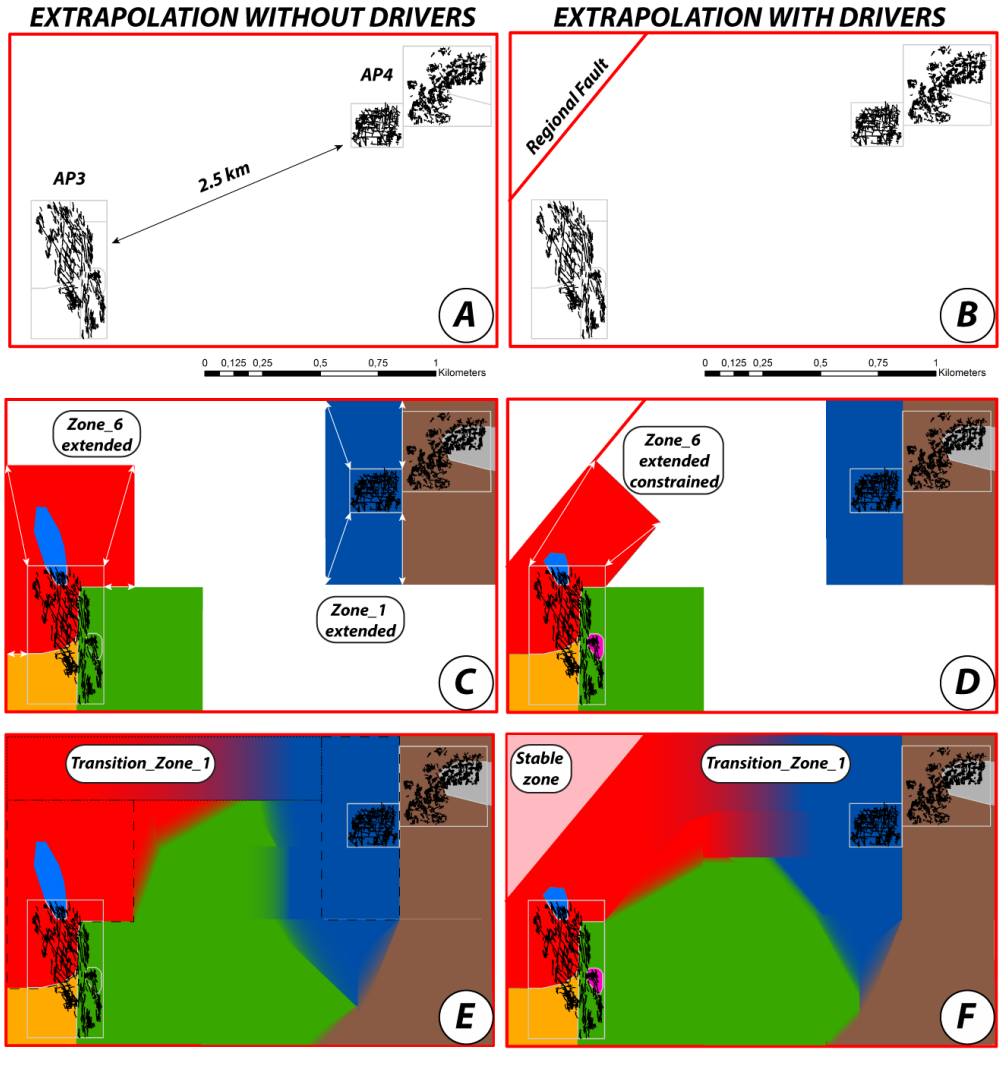
EXTRAPOLATION WITHOUT DRIVERS
EXTRAPOLATION WITH DRIVERS
AP4
AP3
2.5 km
A
Regional Fault
B
0 0,125 0,25 0,5 0,75 1 Kilometers
0 0,125 0,25 0,5 0,75 1 Kilometers
Zone_6 extended
Zone_1 extended
C
Zone_6 extended constrained
D
Transition_Zone_1
E
Stable zone
Transition_Zone_1
F